AD-A038 124 SPECTRA OPTICS SYLMAR CALIF F/G 3/2
EPHEMERAL ACTIVE REGIONS DURING THE SOLAR MINIMUM. I. GENERAL P--ETC(U)
DEC 76 S F MARTIN, K L HARVEY F19628-76-C-0081
UNCLASSIFIED AFGL-TR-76-0255 NL

| OF |
AD
A038124

END

DATE
FILMED
5-77

AFGL-TR-76-0255

12 p.

EPHEMERAL ACTIVE REGIONS DURING THE SOLAR MINIMUM

Part I General Properties and Trends Over the Solar Cycle

Part II Characteristics of Individual Ephemeral Regions

Sara F. Martin
Karen L. Harvey

Spectra Optics
12317 Gladstone Ave.
Sylmar, California 91342

28 December 1976

Final Report for Period 1 October 1975 - 30 September 1976

Approved for public release; distribution unlimited

Prepared for
Air Force Geophysics Laboratory
Air Force Systems Command
United States Air Force
Hanscom AFB, Massachusetts 01731

Unclassified

SECURITY CLASSIFICATION OF THIS PAGE (When Data Entered)

REPORT DOCUMENTATION PAGE

READ INSTRUCTIONS BEFORE COMPLETING FORM

1. REPORT NUMBER: AFGL-TR-76-0255	2. GOVT ACCESSION NO.
3. RECIPIENT'S CATALOG NUMBER	
4. TITLE (and Subtitle): EPHEMERAL ACTIVE REGIONS DURING THE SOLAR MINIMUM. I. General Properties and Trends Over the Solar Cycle. II. Characteristics of Individual Ephemeral Regions.	5. TYPE OF REPORT & PERIOD COVERED: Final Report. 1 Oct '75 - 30 Sep. '76
	6. PERFORMING ORG. REPORT NUMBER
7. AUTHOR(s): Sara F. Martin, Karen L. Harvey	8. CONTRACT OR GRANT NUMBER(s): F19628-76-C-0081
9. PERFORMING ORGANIZATION NAME AND ADDRESS: Spectra Optics, 12317 Gladstone Ave., Sylmar, Calif. 91342	10. PROGRAM ELEMENT, PROJECT, TASK AREA & WORK UNIT NUMBERS: 62101F, 76490613, 06
11. CONTROLLING OFFICE NAME AND ADDRESS: AIR FORCE GEOPHYSICS LABORATORY, Hanscom AFB, Mass. 01731, Monitor/Richard B. Dunn/PH	12. REPORT DATE: 28 December 1976
	13. NUMBER OF PAGES: 56
14. MONITORING AGENCY NAME & ADDRESS (if different from Controlling Office)	15. SECURITY CLASS. (of this report): Unclassified
	15a. DECLASSIFICATION/DOWNGRADING SCHEDULE

16. DISTRIBUTION STATEMENT (of this Report)

Approved for public release; distribution unlimited

17. DISTRIBUTION STATEMENT (of the abstract entered in Block 20, if different from Report)

SK 392 122

18. SUPPLEMENTARY NOTES

19. KEY WORDS (Continue on reverse side if necessary and identify by block number)

Ephemeral active regions, solar cycle, magnetic fields on the sun

20. ABSTRACT (Continue on reverse side if necessary and identify by block number)

General properties of ephemeral active regions were studied using Kitt Peak daily magnetograms from Apr.-Nov. 1975. Although this interval was prior to sunspot minimum, ephemeral regions related to incoming cycle 21 were already more numerous than ephemeral regions related to outgoing cycle 20. The transition between the old and new solar cycle was identified by a reversal of the statistically dominant orientation of regions and sometimes by a minimum in the latitude distribution where adjacent cycles overlapped. During this interval the transition between cycle 20 and 21 was at N18° and S24° deg

next page

DD FORM 1 JAN 73 1473 EDITION OF 1 NOV 65 IS OBSOLETE

Unclassified

SECURITY CLASSIFICATION OF THIS PAGE (When Data Entered)

next → Comparing this 1975 data with previously studied data from 1970 and 1973, we find evidence that incoming cycle 21 was already present on the sun at middle and high latitudes in 1973 and 1970. Extrapolating backward and forward in time from these three periods, we find that it is conceivable that two solar cycles may be present on the sun at all times. It appears that further statistical studies of ephemeral active regions may yield long-term prognostic information on the future course of solar activity.

The birth, development, and decay of individual ephemeral regions were studied from fine-scan magnetograms taken on 1-3 Oct. 1975, 19-22 Nov. 1975, and 17 Jan. 1976 at Kitt Peak Observatory. The Oct. data is characterized by spatial resolution of 0.75" and a low noise level, 2 G/0.75". In this set of data the birth rate of ephemeral regions is 1 per hour per 10^{10} km^2. If this rate is typical of low latitudes, approximately 300 ephemeral regions are born per hour between N30° and S30°.

→ The birth of 90 ephemeral regions was recorded. Prior to the birth of regions, existing network was found to disappear or show lateral displacement. The growth and decay rates of regions were comparable. In the decaying phase, some flux elements simply disappeared; some merged with network or other elements of regions of similar polarity; some collided and simultaneously disappeared with network or elements of other regions of opposite polarity. All clearly identifiable ephemeral regions dissipated by these processes while continuing to expand. Some small adjacent flux elements of opposite polarity appeared to shrink and decay in a manner opposite to the birth of regions. However, in none of these cases were the bipoles observed at birth, an observation which would confirm their identification as ephemeral regions. Hence, no positive evidence was found by which any subset of ephemeral regions could be interpreted as being a phenomenon different from active regions.

Preface

This study constitutes further research on the subject of ephemeral active regions which was initiated under AFCRL Contract F19628-73-C-0184 by the present authors when they were employed at the Lockheed Solar Observatory by the Lockheed Missiles and Space Co. The titles of the previous publications are: Ephemeral Active Regions (Harvey, K. L., and Martin, S. F. (1973), Ephemeral Active Regions in 1970 and 1973 (Harvey, K. L., Harvey, J. W. and Martin, S. F., 1975).

The authors thank B. Gillespie and J. W. Harvey for their assistance in acquiring new obeervations during 1975 and 1976 and of L. Myers for programming and plotting the random distributions of active regions in longitude.

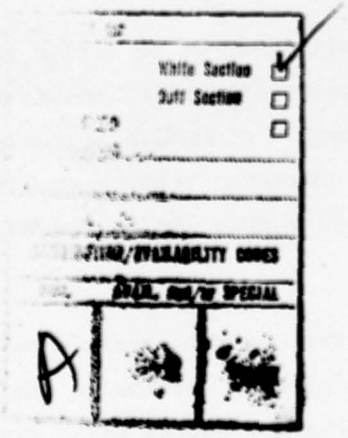

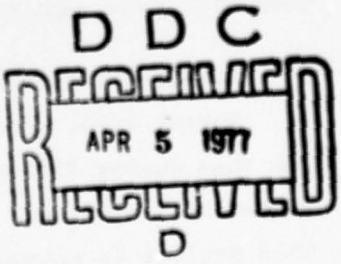

EPHEMERAL ACTIVE REGIONS DURING THE SOLAR MINIMUM

Part I - General Properties and Trends over the Solar Cycle

1. INTRODUCTION

A study of ephemeral active centers occurring on the sun during solar minimum was initiated to collect more information on how the number of ephemeral regions varies as a function of time during the solar cycle, to determine the approximate number present on the whole sun at any time during the solar minimum, and to test our ability to differentiate between ephemeral regions associated with incoming solar cycle from those associated with declining solar cycle.

In this section we report on the statistical properties of ephemeral regions occurring during six months of the current solar minimum and compare these results with previous studies of ephemeral region data from periods of similar length in 1970 and 1973 (Harvey, Harvey & Martin, 1975). The data studied includes all ephemeral active regions and active regions identifiable on the Kitt Peak daily magnetograms and/or listed in the McMath Calcium Plage tables in Solar Geophysical Data, from April to November 1975. However, no Kitt Peak magnetograms were available from August 10 to October 2, 1975. Hence, the period studied is representative of a 6 month rather than an 8 month interval during the solar minimum.

The McMath plage tabulations included a small fraction of active regions with lifetimes of only one day which were also identified as ephemeral regions on the Kitt Peak magnetograms. This redundant sample of McMath ephemeral regions was removed from our new tabulations of ephemeral regions compiled from Kitt Peak magnetograms to make the data samples mutually exclusive.

2. NUMBER DISTRIBUTION AS A FUNCTION OF TIME

During 1975, substantially fewer ephemeral regions were visible on the sun than during 1973 or 1970 consistent with the general decline in the total number of long-lived, sunspot-producing, active regions during solar cycle 20. This decline in ephemeral regions is graphically illustrated in Fig. 1 in comparison with the sunspot numbers for solar cycle 20. The sunspot numbers are the smoothed daily Zurich sunspot numbers as published in Solar Geophysical Data.

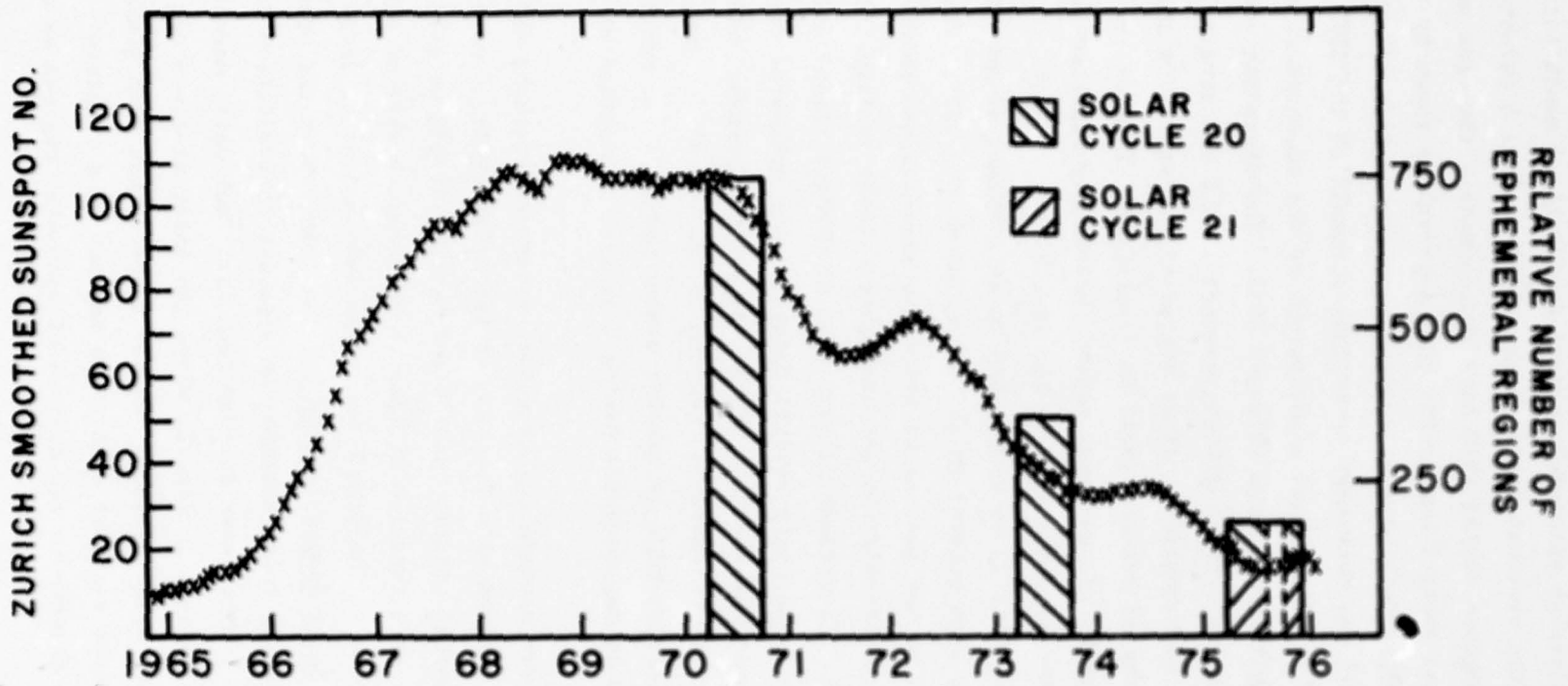

Fig. 1. Relative number of ephemeral active regions occurring on average at any one time on the whole sun in comparison with the Zurich smoothed sunspot number.

The relative number of ephemeral regions during the 6 month intervals studied is given on the vertical scale on the right in Fig. 1 selected such that the ephemeral regions during 1970 have approximately the same amplitude as the Zurich Smoothed sunspot number for that interval as shown by the vertical coordinate on the left. To arrive at correct relative numbers of ephemeral regions for Fig. 1, it was necessary to degrade a sample of the 1975 magnetograms taken with 512 channel magnetograph to the apparent resolution of the 40 channel magnetograms from 1970 and 1973. The degrading was accomplished by averaging every 4 picture elements, in 2 x 2 arrays, across a sample of 10 daily magnetograms. After degrading, it was found that a factor 2.1 fewer ephemeral regions could be identified. This factor was then multiplied by the numbers of ephemeral regions previously reported for 1970 and 1973 to arrive at comparable numbers for Fig. 1.

As illustrated in Fig. 1, we found that on an average, at any given time, 182 ephemeral regions were present on the whole sun during 1975. This number is strongly dependent on the quality of the daily magnetograms which is a function of instrumental resolution and atmospheric image quality. In fine-scan magnetograms, taken during periods of very good atmospheric image quality, we find that we are able to identify several times as many ephemeral regions per unit area than on comparable sections of the daily magnetograms. Hence, there may easily be as many as 500 ephemeral regions on the sun at any time during solar minimum and a correspondingly greater number during solar maximum which would be identifiable in magnetograms having a spatial resolution of about 1 arc sec.

Our previous papers contain contradictory evidence regarding the changing numbers of ephemeral regions as a function of the solar cycle. In our initial investigation of ephemeral regions (Harvey and Martin, 1973), we prepared a graph showing changes as a function of time in the small sample of ephemeral active regions contained in the McMath Ca plage tabulations of large active regions published in Solar Geophysical Data. The graph shows the ephemeral regions to maximize during solar minimum, an apparent contradiction to the results shown in Fig. 1 which were derived from Kitt Peak daily magnetograms. This discrepancy is also seen in Fig. 2, where the shortest-lived regions seem to be increasing toward solar minimum. We now suspect that each graph may contain valid information and that each graph may not be a complete representation of the changes in the numbers of ephemeral regions as a function of time.

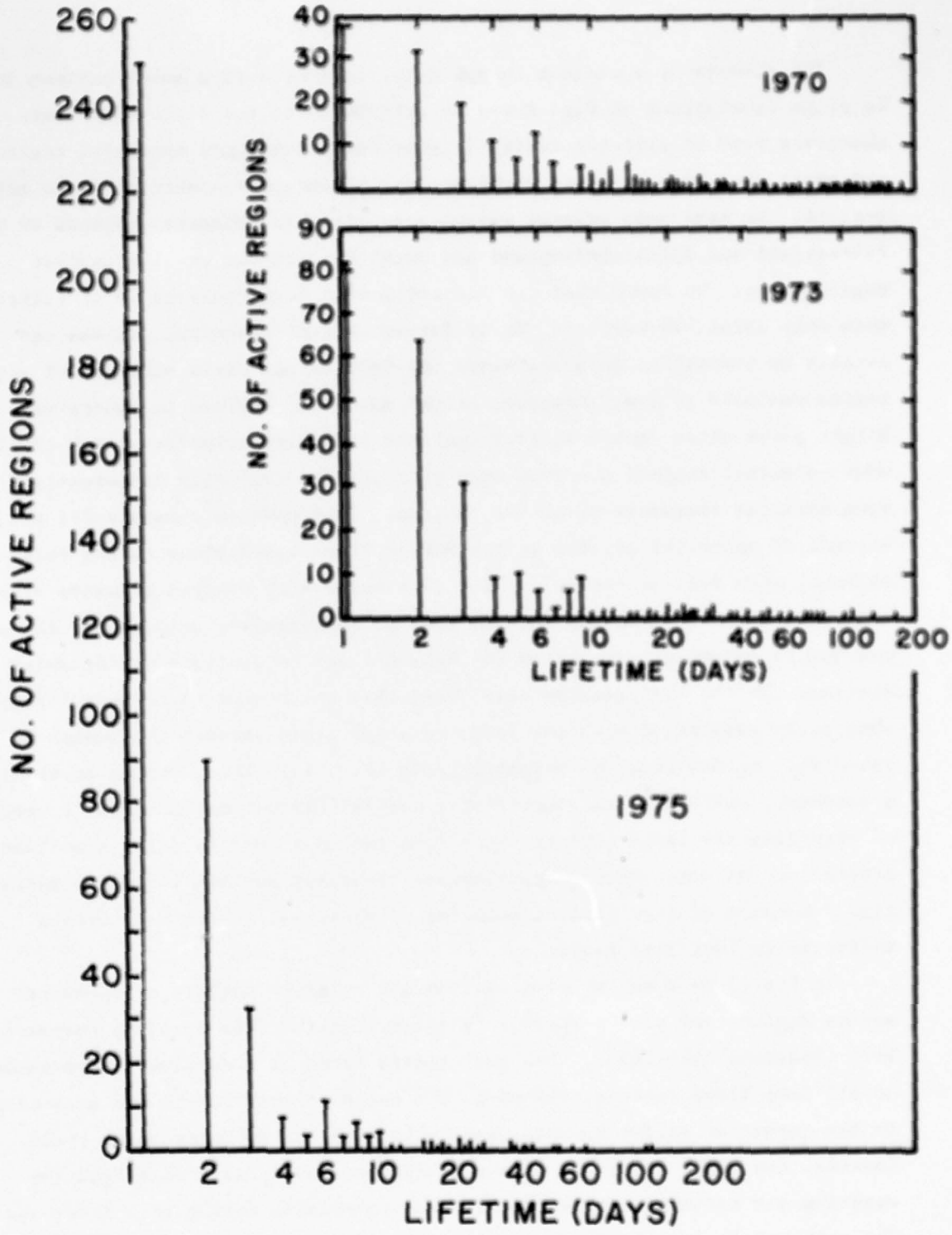

Fig. 2. Lifetime distribution of active centers (regions) as determined from calcium plage data tabulated at McMath-Hulbert Observatory and published in Solar Geophysical Data. The intervals illustrated are Apr.-Sep. 1970, 1973, and 1975. The 1975 data has been corrected to identify only single bipolar magnetic field units as seen on the daily magnetograms from Kitt Peak Observatory.

The absence of a maximum in ephemeral regions during solar maximum in the Ca plage tabulations in Fig. 2 can be attributed to the difficulty that observers face in differentiating between newly developed ephemeral regions and small clumpings of plage which are the dispersed remnants of large active regions. We have made several attempts to identify ephemeral regions on Ca II filtergrams and spectroheliograms and later checked our results against magnetograms. We found that our identification based only on Ca II filtergrams were only about 50% correct. Newly formed, bright ephemeral regions can usually be identified in areas where the density and field strength of active region remnants is low. However, bright ephemeral regions in moderately bright plage often cannot be distinguished from tiny unipolar clumps of plage. Weak ephemeral regions are even more difficult to correctly differentiate from unipolar fragments of active regions. This problem accounts for the absence of ephemeral regions in the McMath Plage tabulations during solar maximum, when most of the solar disk is covered with decayed remnants of active regions. However, this explanation does not necessarily account for the apparent maximum in ephemeral regions in the McMath Plage tabulations during solar minimum. In the 1975 data we have found that the number of ephemeral regions apparently associated with the incoming solar cycle exceeds the number of ephemeral regions from the outgoing cycle (Fig. 1). Thus, during solar minimum, a secondary maximum in the number of ephemeral regions may occur as a result of significantly large contributions from two solar cycles being simultaneously present on the sun. Such a hypothesized secondary maximum would not appear in Fig. 1 because of insufficient sampling of ephemeral region data over a sufficiently long time base.

In Fig. 3 we show the distribution and relative numbers of ephemeral active regions and active regions by solar rotation from April to November 1975 (Rotation 1626-1635). The anticipated trend is a decline in the number of all long-lived regions related to the outgoing solar cycle and an incline in the number of active regions associated with the incoming solar cycle. However, the total number of ephemeral regions, associated with both the outgoing and incoming cycles, seems to be increasing during this interval. The increase in incoming cycles regions is not surprising since new cycle sunspots were also beginning to appear. However, the apparent increase in outgoing cycle ephemeral regions was not expected. This may be due simply to a temporary fluctuation in the sunspot numbers during this interval. A very

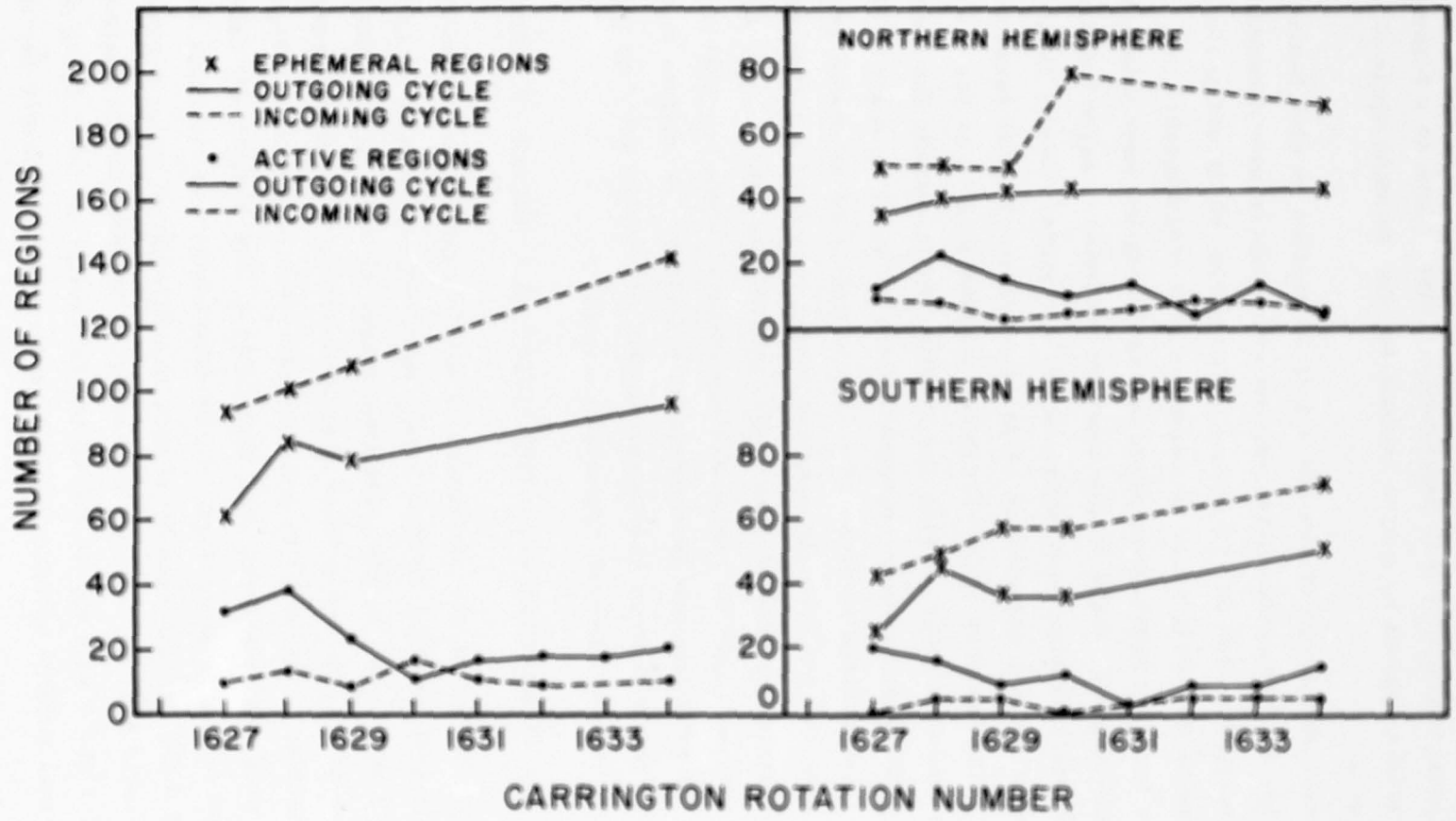

Fig. 3. Number of ephemeral and long-lived magnetic regions per solar rotation from Apr.-Nov. 1975. Northern and southern hemispheres are shown combined on the left and separately on the right.

surprising result is that the new cycle ephemeral regions outnumber the old cycle ephemeral regions in both hemispheres. Thus, there is a higher ratio of ephemeral active regions to active regions for the incoming cycle than the outgoing cycle.

The relative numbers of new and old cycle regions in each hemisphere is shown in Fig. 3. New cycle active regions are slightly more numerous in the northern hemisphere than in the southern hemisphere, while old cycle active regions seem to be nearly equal in number in both hemispheres.

In the northern hemisphere, major new cycle regions have caught up with the old cycle regions, while in the southern hemisphere, major incoming cycle regions are still lagging major outgoing cycle regions. Hence, it is evident that the solar minimum measured in terms of traditional solar parameters must take place after November 1975. The solar minimum, defined as the time when the sunspot number associated with the incoming cycle exceeds the number associated with outgoing cycle, occurred around or after December 1975. However, a solar minimum in terms of relative numbers of ephemeral regions associated with the incoming and outgoing cycles must have occurred sometime prior to the beginning date of this study, probably in late 1974 or early 1975. This means that an ephemeral region minimum occurred about one year or more in advance of the solar minimum as traditionally defined. We suggest that valuable prognostic information about the course of the solar cycle activity <u>may</u> by found through the continued study of ephemeral regions.

3. VARIATIONS IN EPHEMERAL AND ACTIVE REGIONS AS A FUNCTION OF LIFETIME

The distribution of the lifetimes of active regions for the months of April-October 1975 is shown in Fig. 2 in comparison with similar graphs for 1970 and 1973 data. Due to the continuous nature of these distributions and other reasons cited previously (Harvey et al., 1975), we consider ephemeral regions to be simply the smallest and shortest-lived of all active regions.

As expected, it is evident that long-lived active regions ($\gtrsim$4 days) are more numerous during solar maximum. It is surprising, however, that the number of 2 day and 3 day regions seem to be more numerous during solar minimum (1975) than during solar maximum (1970). This apparent increase in the regions having lifetimes of 2 and 3 days may be due to the difficulty in identifying short-lived regions at times outside of solar minimum as discussed previously for ephemeral

regions (1 day lifetimes). To be certain of this probable explanation, however, identifications of short-lived regions should be made using daily (or more frequent) magnetograms throughout a whole solar cycle.

4. ORIENTATION

The identification of incoming cycle and outgoing cycle active regions is traditionally made on the basis of the relative orientation of opposite polarities within a region. For ephemeral active regions, however, this criteria is valid only for large statistical samples. This is due to the fact that the relative orientation of the opposite polarities varies a function of lifetime as seen on Fig. 4. For regions with lifetimes $\gtrsim 3$ days, the shorter the lifetime, the more likely it is that the orientation of the bipole will be random. Conversely, the longer the lifetime, up to about 3 days, the more likely a region will possess (for most of its lifetime) the same orientation possessed by the majority of sunspots groups for the cycle and hemisphere in which the sunspots appear. On longitudinal magnetograms, the orientation of active regions, ephemeral regions or sunspots can be established by drawing a line from the centroid of the peak of one polarity to the centroid of the peak field of opposite polarity. In this paper, we arbitrarily define the direction as going from positive to negative and identify the direction with an arrow. The angle that this arrow has with respect to a line parallel to the solar equator establishes the orientation of the primary bipolar components of a region. To simplify the task of determining orientation for thousands of ephemeral regions, all regions were visually divided into 8 orientation bins each 45° wide with the bin boundaries being the same as the 8 points on a compass with solar coordinates: N, NE, E, SE, S, SW, W, and NW. With this system we could rapidly visually estimate and tabulate the orientation of all ephemeral and active regions in this study for which magnetic field information was available.

The orientations which follow the Hale Law of sunspot polarities for the current solar cycles also are shown on the left side of Fig. 4. It is seen in Fig. 4 that almost all regions having lifetimes greater than 2 days have proper orientations according to the Hale Law. Regions having lifetimes of 2 and 3 days tend to have more proper than reverse orientations. Ephemeral regions have nearly random orientations with only a slight tendency to favor the proper orientations of the cycle and hemisphere in which they occur. It is also seen

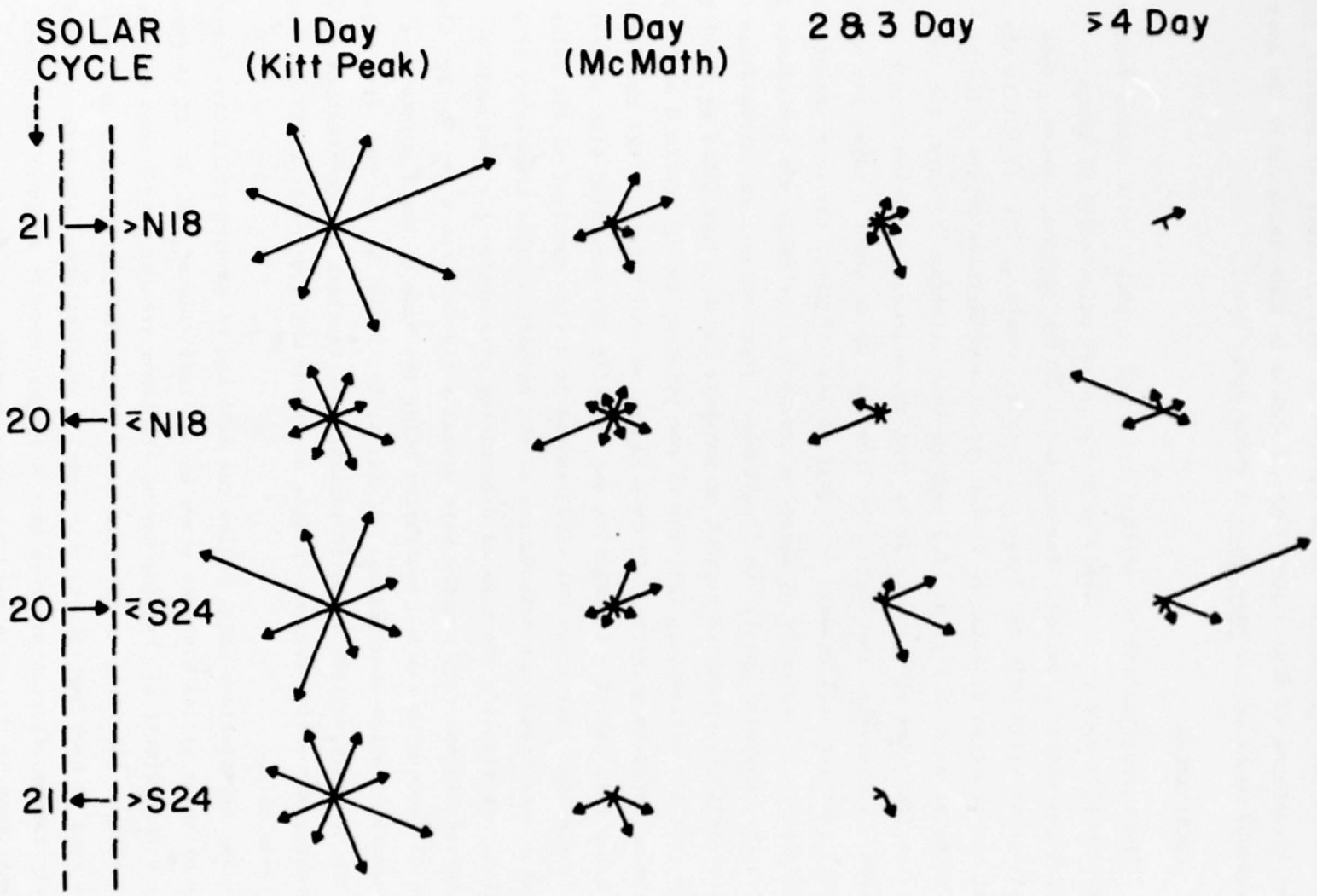

Fig. 4. Orientation of active regions for various lifetime groupings. Vectors point from positive to negative polarity in solar coordinates. Most regions whose lifetimes are 1 day follow the orientation pattern known as the Hale law of sunspot polarities. Arrows on the left show the dominant orientation for sunspot producing regions according to the Hale law for solar cycle 20 at low latitudes and for solar cycle 21 at high latitudes.

that the high latitude cycle 21 regions of 2 and 3 day lifetimes tend to be more randomly oriented than the 2 and 3 day regions from established cycle 20. A likely explanation for this difference is that high latitude, cycle 21 regions may tend to be shorter-lived on average than low latitude regions.

From a study by Weart (1970) we know that even long-lived regions initially appear with random orientations and that the proper orientations according to the Hale Law are usually established in the first day of development. Thus, by comparison, with the ephemeral regions, we can surmise that the orientation behavior of any active regions in its first or second day may be an indicator of how long-lived the region will ultimately be. The behavior of all active regions in their first day of development is a subject which should be studied further with high resolution telescopes.

5. DIFFERENTIATING BETWEEN SUCCESSIVE SOLAR CYCLES

From the above, it is obvious that we cannot identify individual new cycle ephemeral regions from individual old cycle ephemeral regions based on the relative orientation of opposite polarities. However, the statistical trends of a large sample of ephemeral regions as a function of latitude and as a function of orientation do allow us to identify ephemeral regions associated with both the incoming and outgoing solar cycles. In Fig. 5, we show the latitude distributions for 4 groups of active regions: long-lived, 54 days; short-lived 2-14 days; 1 day (ephemeral) regions from the McMath Ca Plage tabulation; and 1 day (ephemeral) regions tabulated from the Kitt Peak daily magnetograms, exclusive of the 1 day McMath regions.

Both groups of ephemeral regions show maxima in these distributions corresponding to outgoing solar cycle 20 within 12° north and south of the solar equator and maxima corresponding to developing solar cycle 21 around 37° north and south latitude. For outgoing cycle 20, the ephemeral region maxima correspond to the maxima in the latitude distribution of long-lived regions. However, for the incoming cycle, the ephemeral region maxima tend to be at higher latitudes than the maxima in the regions with lifetimes equal to or greater than 2 days (Fig. 5).

The long-lived regions show little evidence of the incoming solar cycle while the short-lived regions show substantial numbers of regions associated with the incoming solar cycle. Ephemeral region maxima associated with the incoming cycle are nearly equal to the maxima associated with the outgoing cycle.

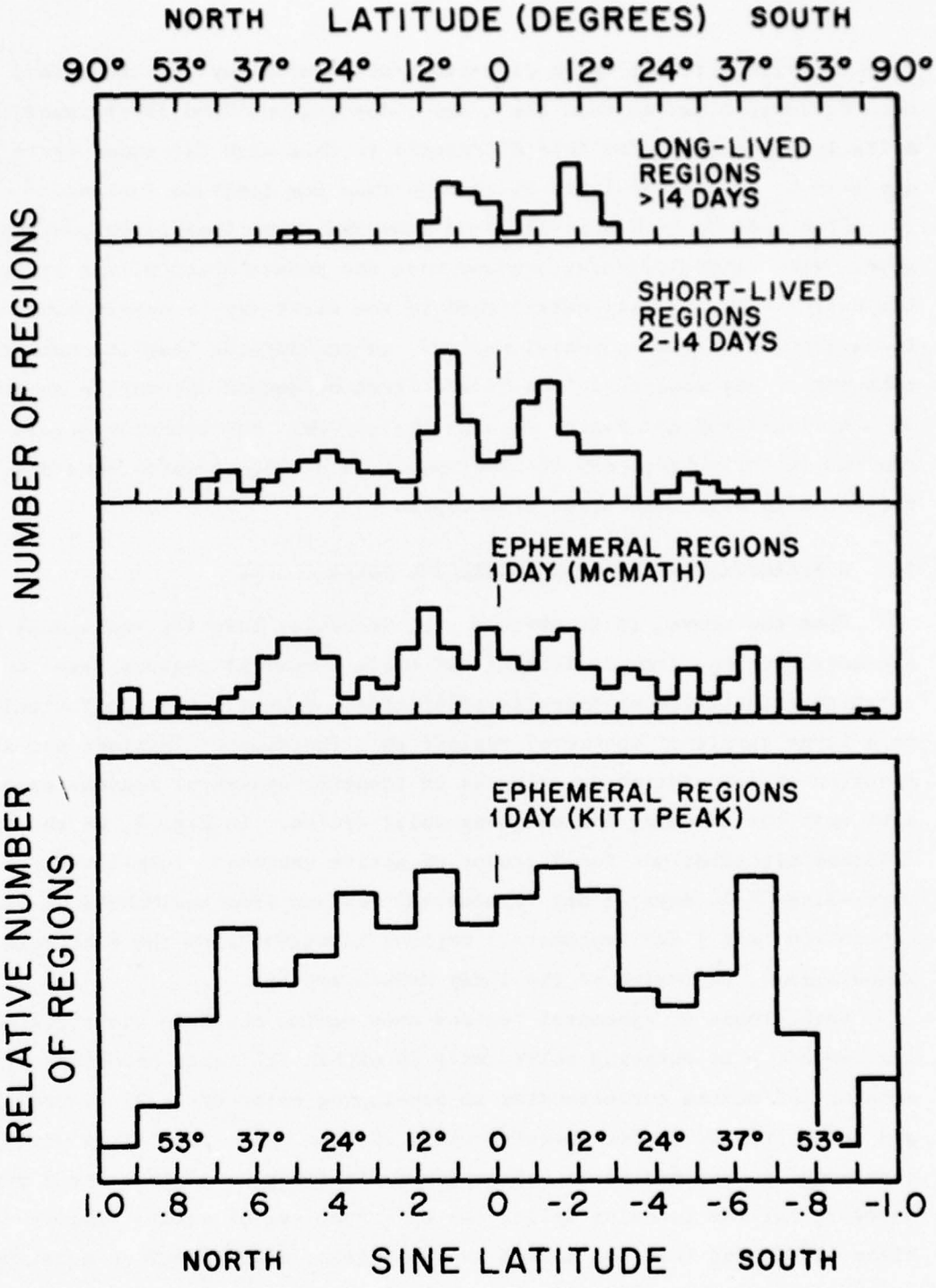

Fig. 5. Distribution in latitude for active regions in several lifetime grouping for Apr.-Nov. 1975. Mid-latitude peaks corresponding to incoming solar cycle 21 increase in amplitude with shorter lifetimes more rapidly than do regions associated with outgoing cycle 20.

This trend merely illustrates the well known fact that the earliest regions to appear in a new solar cycle are usually short-lived. It is an important point to reiterate, however, because it is now evident that further study of ephemeral regions may yield long-term prognostic information about future course solar cycles. Consequently, it is also important to know how well we can statistically identify ephemeral regions with a particular solar cycle.

The new cycle and old cycle components of ephemeral regions are usually distinguishable in data samples as short as 1 solar rotation. In Fig. 6, ephemeral regions for solar rotation numbers 1627 through 1635 are shown excluding rotations 1631 and 1632 because insufficient data were obtained in these rotations. Also, rotations 1633 and 1635 were incompletely sampled. Rotations 1627, 1628, 1629, 1630, 1633, 1634, and 1635 show distinct high latitude maxima between 30° and 44° south in either or both the northern and southern hemisphere. All four maxima, however, do not necessarily appear clearly in data samples taken during a single solar rotation.

The two incoming and two outgoing cycle maxima can be seen more clearly when the entire data sample is divided between regions having the proper orientations (conforming to the Hale Law for sunspots for cycle 20) and reverse orientations as illustrated in Fig. 7. Subtracting the reverse orientations from the proper orientations as in Fig. 8 more clearly shows the statistical tendency for ephemeral regions to conform to the Hale Law for sunspot polarities and hence differentiates outgoing cycle from incoming cycle regions.

On the basis of the minima in the latitude distribution between regions associated with the incoming and outgoing cycles, as well as on the reversal of the majority of regions in orientation at these minima, we have found for the northern hemisphere that the incoming cycle regions are more numerous north of 18° and outgoing cycle regions are more numerous equatorward of 18°. For the southern hemisphere, the transition between incoming cycle regions and outgoing cycle regions is at approximately 24° south latitude as illustrated by the distribution in Fig. 9. The apparent broadening of the latitude distribution of active regions, when considering active regions of successively shorter lifetimes, suggests to us that there is probably no sharp cutoff between regions associated with the incoming and outgoing solar cycles. The distributions of ephemeral regions and short-lived regions from adjacent solar cycles seem to spatially overlap. This property is difficult to reconcile with the Babcock (1961), Leighton (1969) and Parker (1970) dynamo models of the solar cycle.

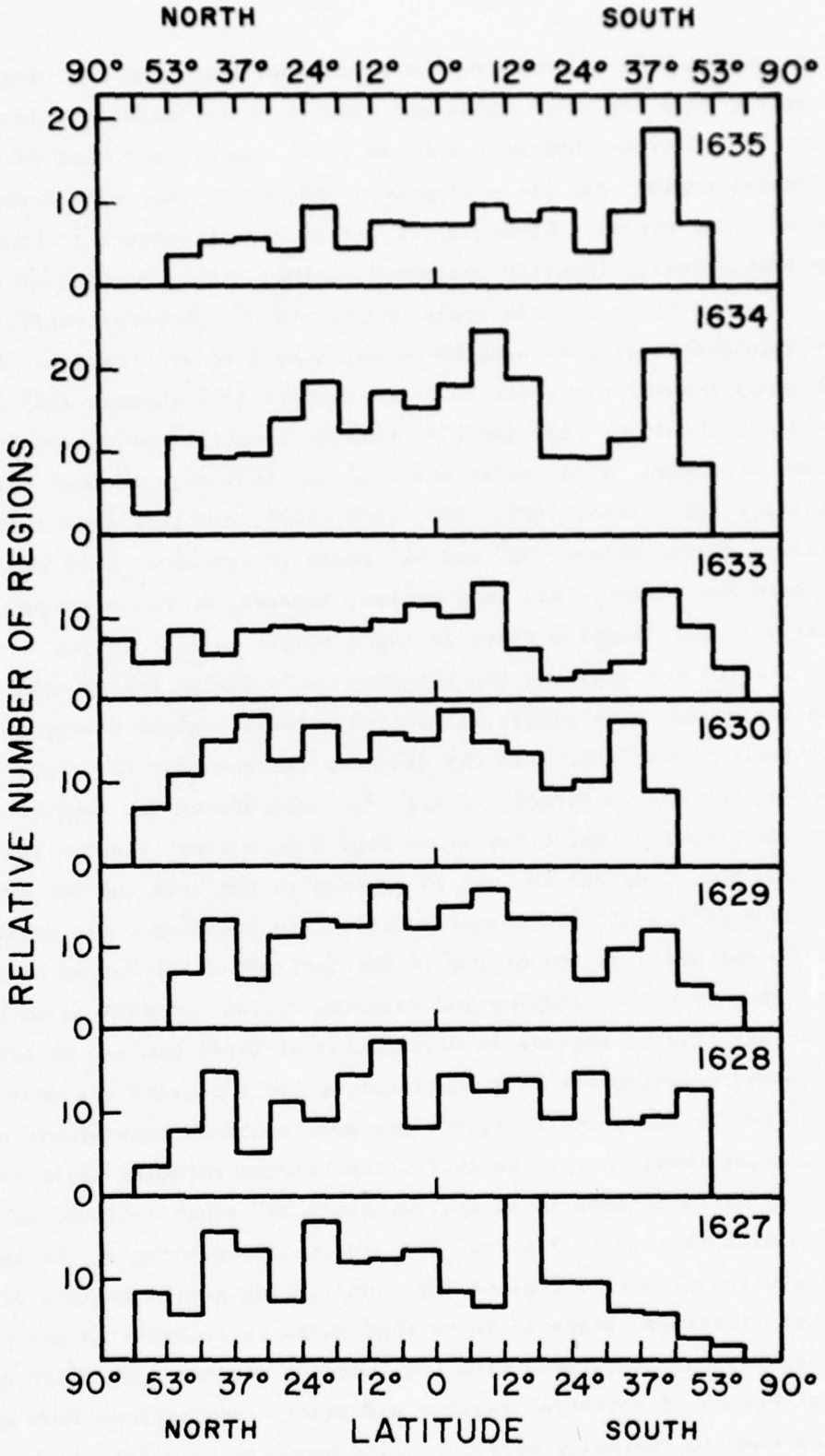

Fig. 6. Latitude distribution of ephemeral active regions by solar rotation from Apr.-Nov. 1975.

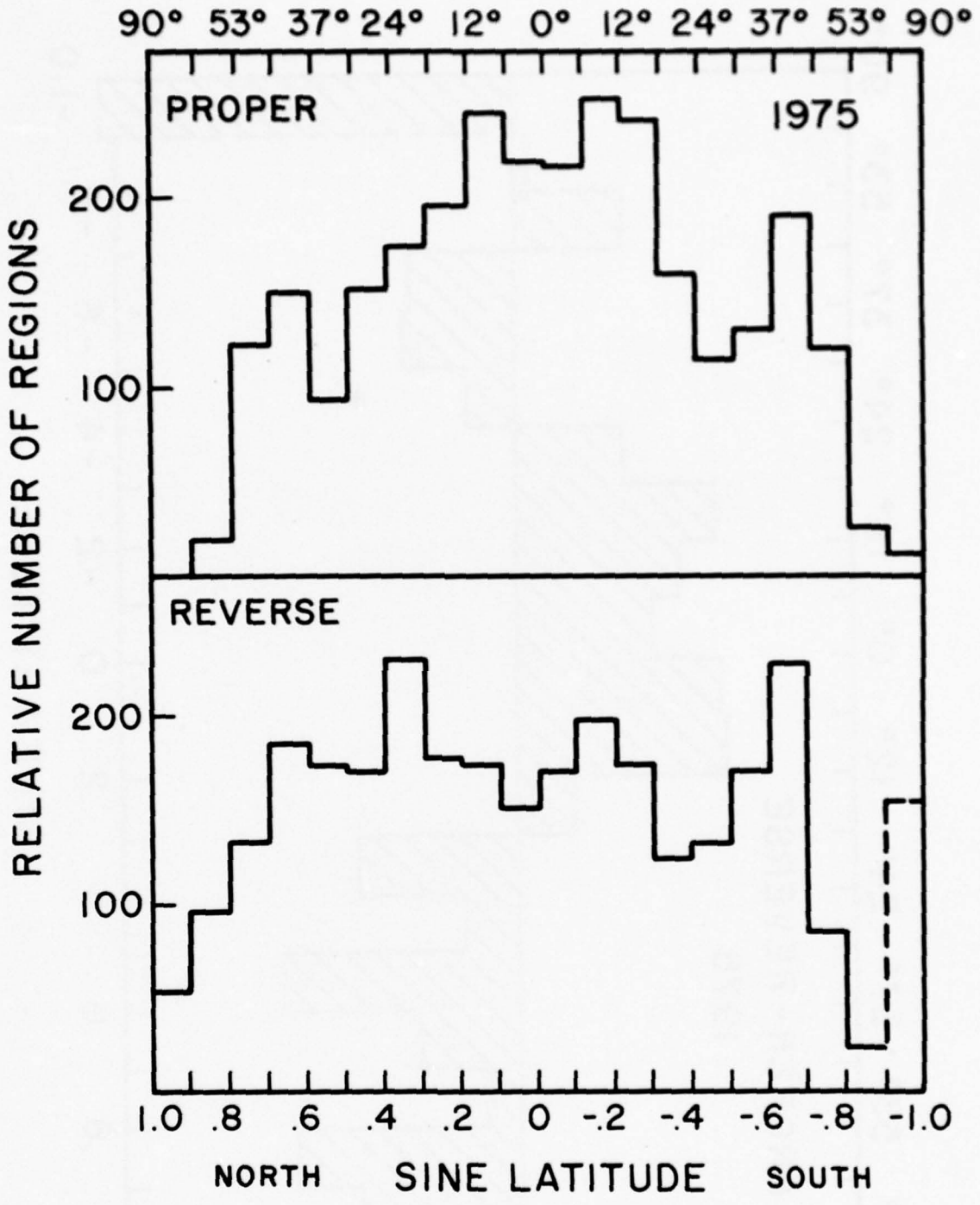

Fig. 7. Latitude distribution of ephemeral active regions separated into two categories: proper - those having the same orientations as exhibited by sunspot regions in cycle 20; reverse - those having opposite orientations to the sunspot producing regions of cycle 20.

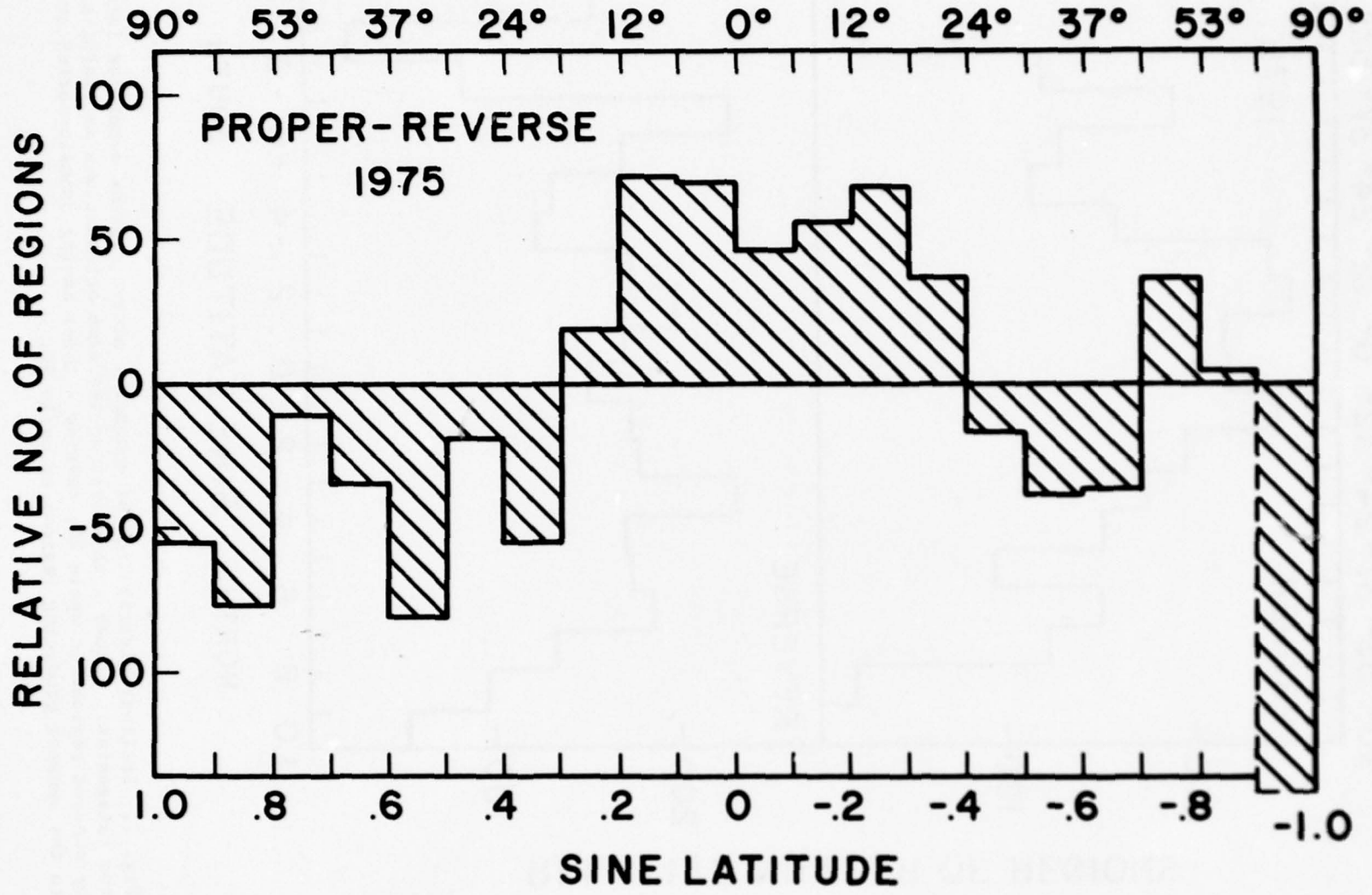

Fig. 8. A subtraction of the 'proper' and 'reverse' categories of ephemeral active regions shown in Fig. 7. The dominant orientation is 'proper' equatorward of N18 and S24 and 'reverse' above these latitudes.

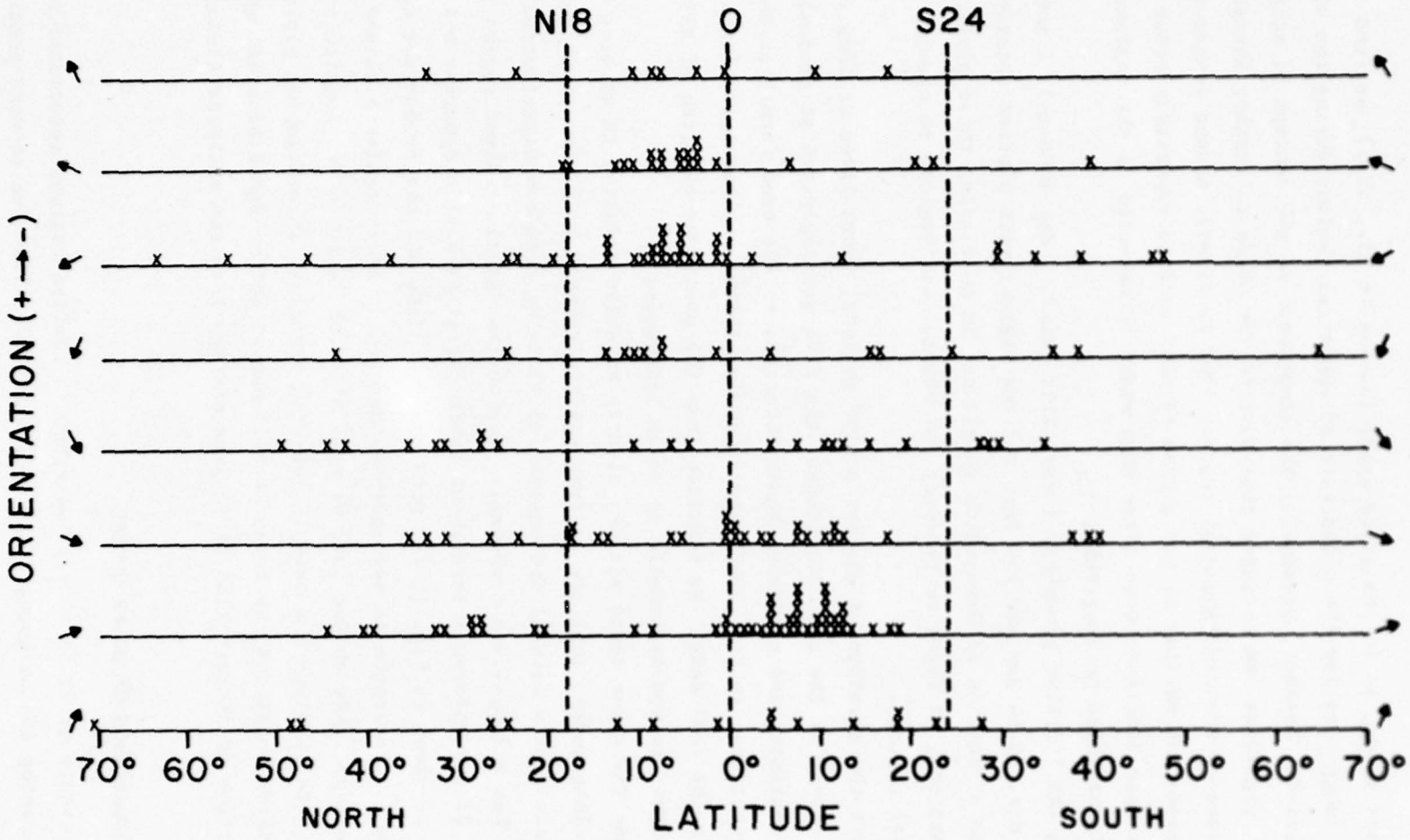

Fig. 9. Latitude distribution of all active regions with known orientations as determined from Kitt Peak daily magnetograms from Apr.-Nov. 1975. Each horizontal line includes all regions with orientations within 22.5° of the direction indicated by the arrow. The majority of regions possess opposite orientations on either side of the dashed lines at N18 and S24. Hence, these are the transition latitudes separating the majority of incoming cycle 21 regions from the majority of outgoing cycle 20 regions.

6. DISTRIBUTION OF ACTIVE REGIONS IN LONGITUDE

In this study, as in the prior study (Harvey et al., 1975), we find no preferred longitudes for the occurrence of ephemeral regions during the six months studied. However, because of the importance of the concept of active and quiet longitudes, we extended this part of the study to further investigate the questions of whether ephemeral regions tend to cluster around longer-lived active regions and whether or not active regions tend to repeatedly occur at nearly the same longitude more often than would be expected if the regions were randomly distributed in longitude.

Using the lifetime groupings 1 day (Kitt Peak), 1 day (McMath), 2 and 3 day, 4-14 day, 15-54 day and >54 day, all the regions were plotted rotation by rotation as a function of Carrington longitude. In overlaying these plots in all combinations, we found no tendency for short-lived regions to cluster around longer-lived regions.

To test the question of whether active regions, short-lived or long-lived, repeatedly occur at the same longitudes, the data was replotted at randomly selected longitudes and randomly chosen rotations in the same format as the real distribution. In Fig. 10-14 the randomly plotted regions are shown adjacent to the real data. We conclude that the positions of birth of all active regions are non-systematic in solar longitude.

Because the above tests yielded clearly negative results, it appears that the active longitudes, that are so frequently displayed in 27 day recurrence diagrams, are just a natural consequence of plotting a random distribution of data which has a long-lived component. Replotting each long-lived region in Fig. 14 at 27 day intervals throughout their lifetimes yields apparent active longitudes as shown in Fig. 15 for both the real data and the randomized data.

As one further check to see whether there could be irregularly shaped, unusually active zones on the sun, we made plots of latitude vs. longitude displaying both lifetime and orientation with symbols. In overlaying plots from successive rotations, we found no evidence of active zones or areas where the orientation or distribution of regions differs from the patterns already discussed.

7. THE PROGRESSION OF SOLAR CYCLES

The presence of large numbers of ephemeral active regions associated with both the incoming and outgoing solar cycles in 1975 allows us to make predictions

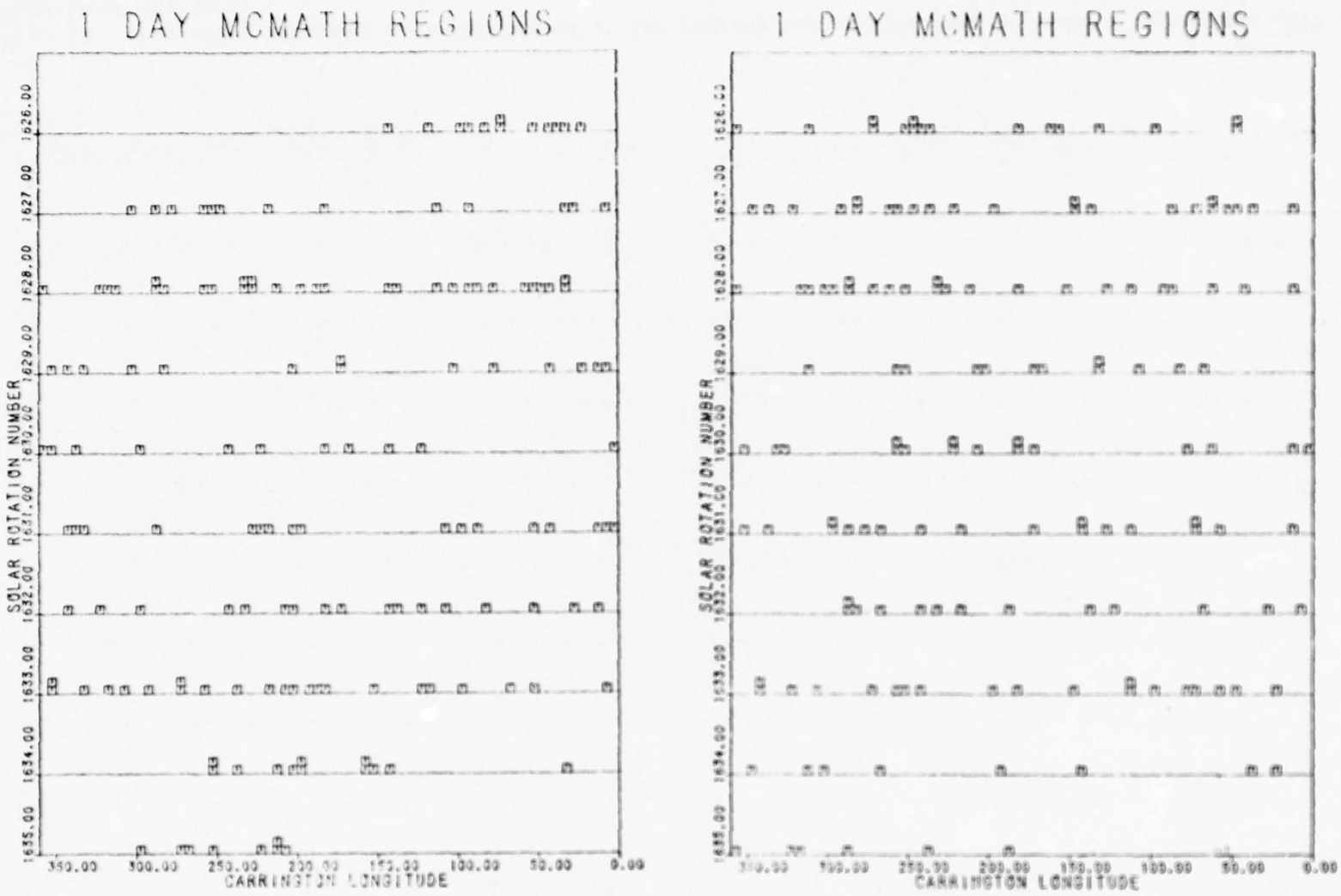

Fig. 10. Longitude distribution of McMath-Hulbert Observatory tabulations of calcium plages having a lifetime of 1 day and a randomized redistribution of the same data. The real data is at the left.

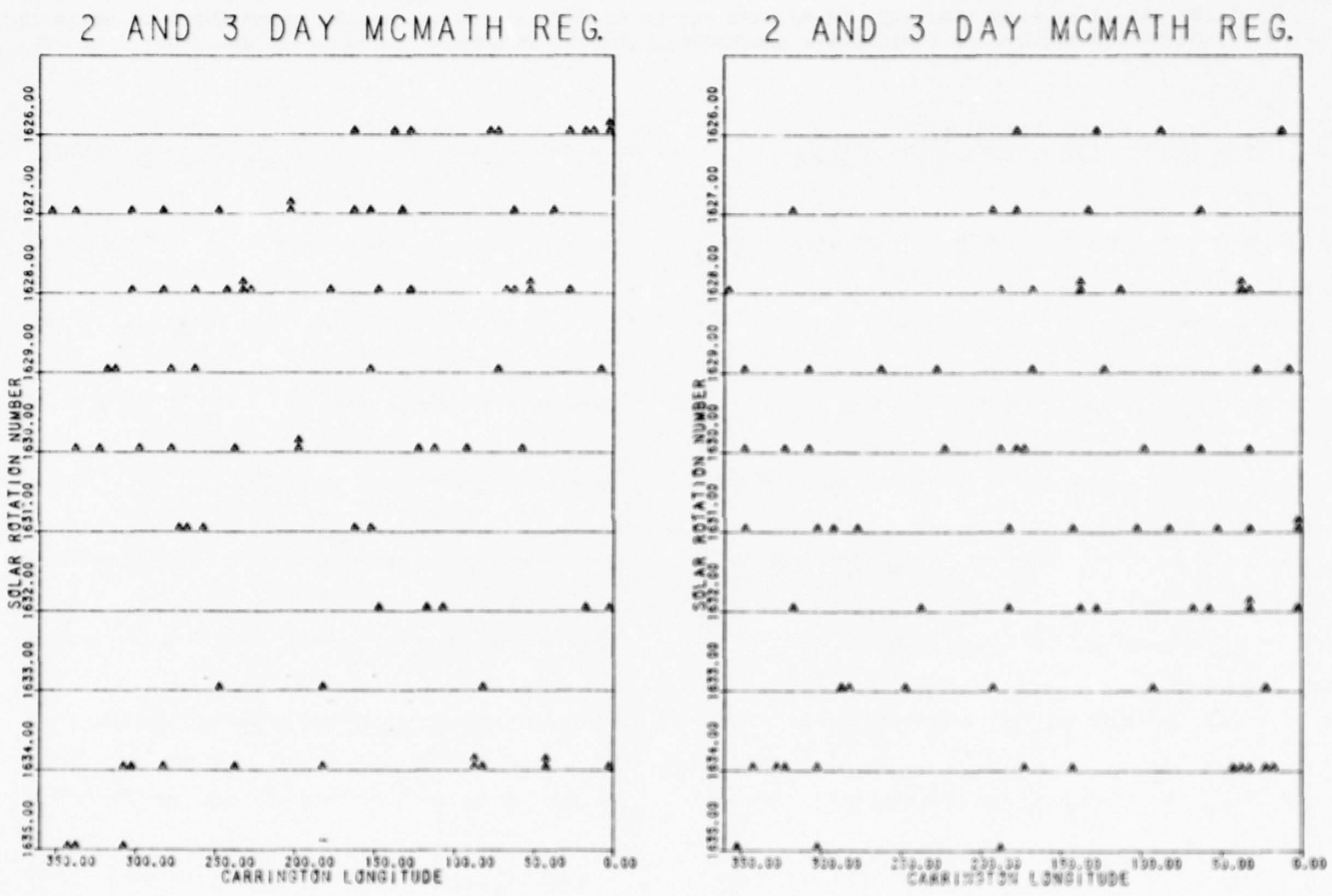

Fig. 11. Real and randomized distributions of active regions having lifetimes of 2 and 3 days. The real data is at the left.

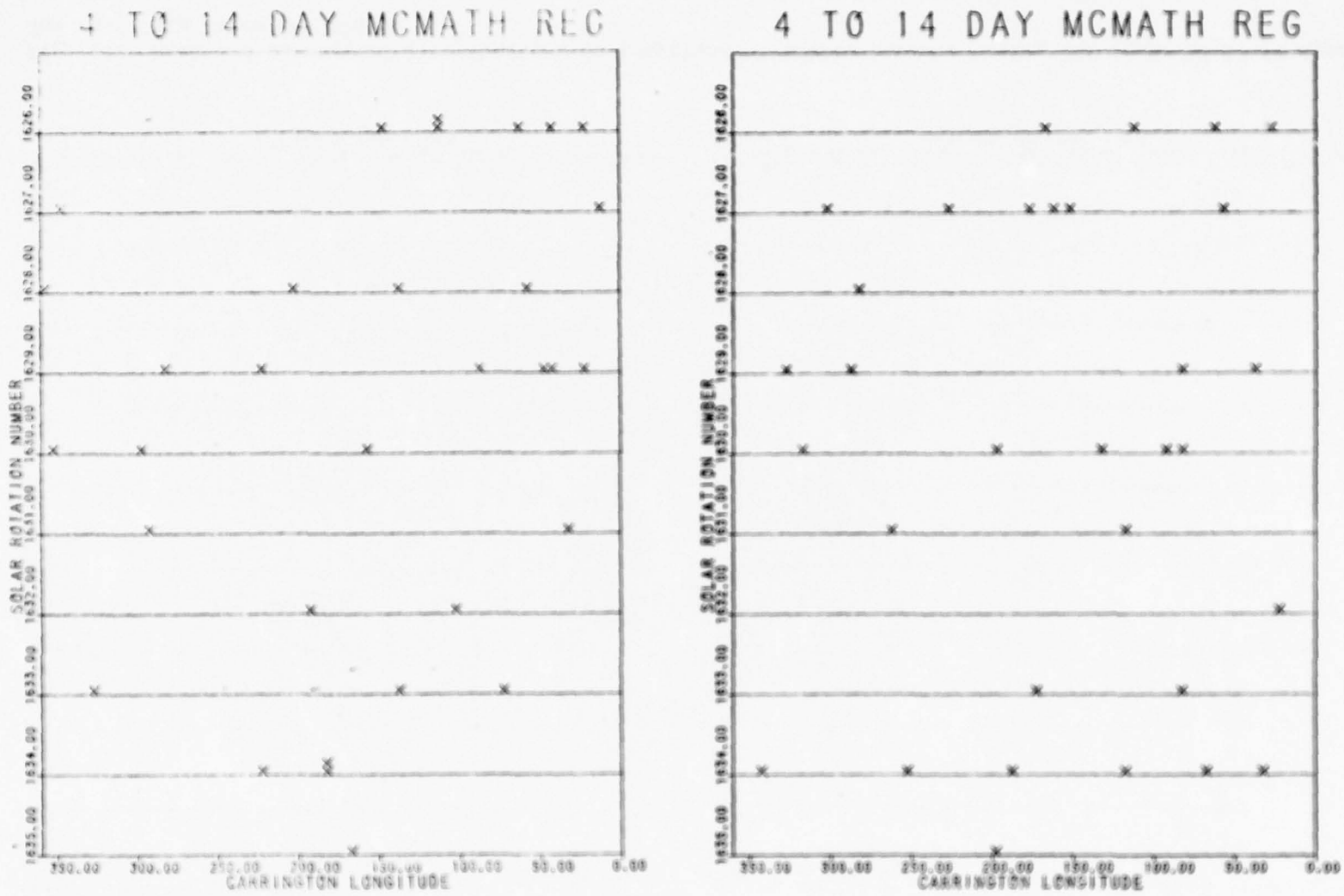

Fig. 12. Real and randomized distributions in longitude of active regions having lifetimes of 4-14 days. The real data is on the right.

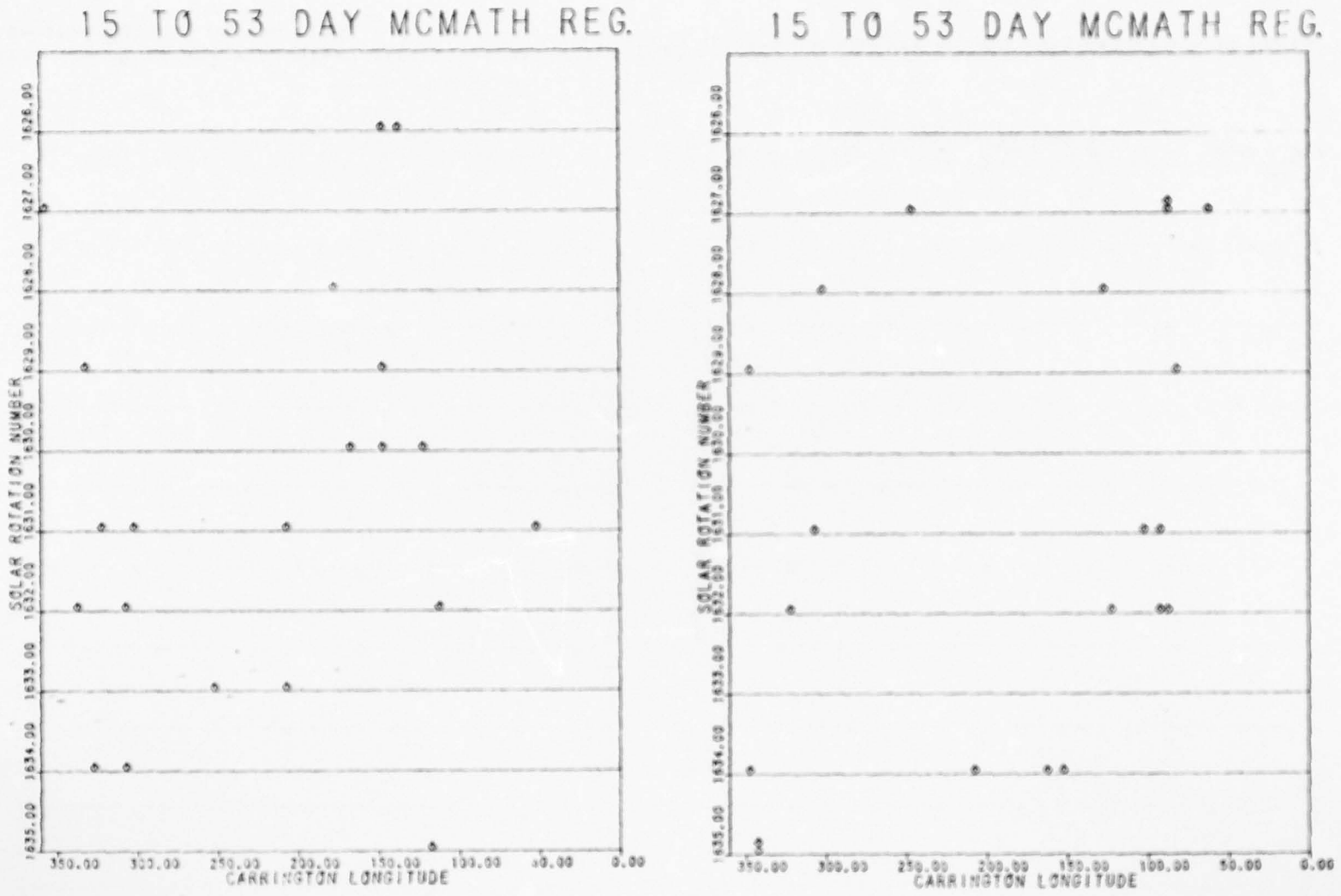

Fig. 13. Real and randomized distributions in longitude of active regions having lifetimes of 15-53 days. The real data is on the right.

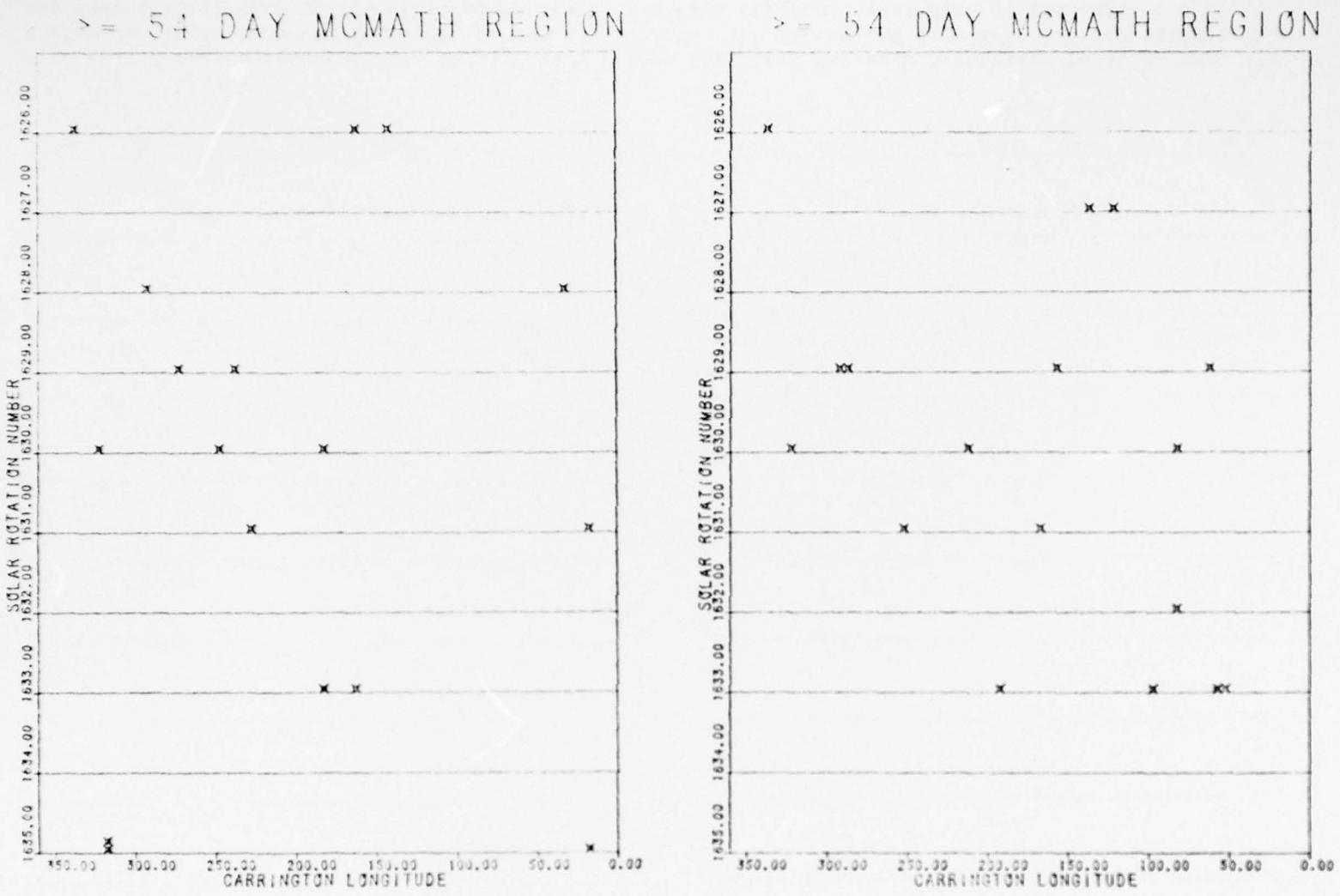

Fig. 14. Real and randomized distributions in longitude of active regions having lifetimes of 54 days. The real data is on the right.

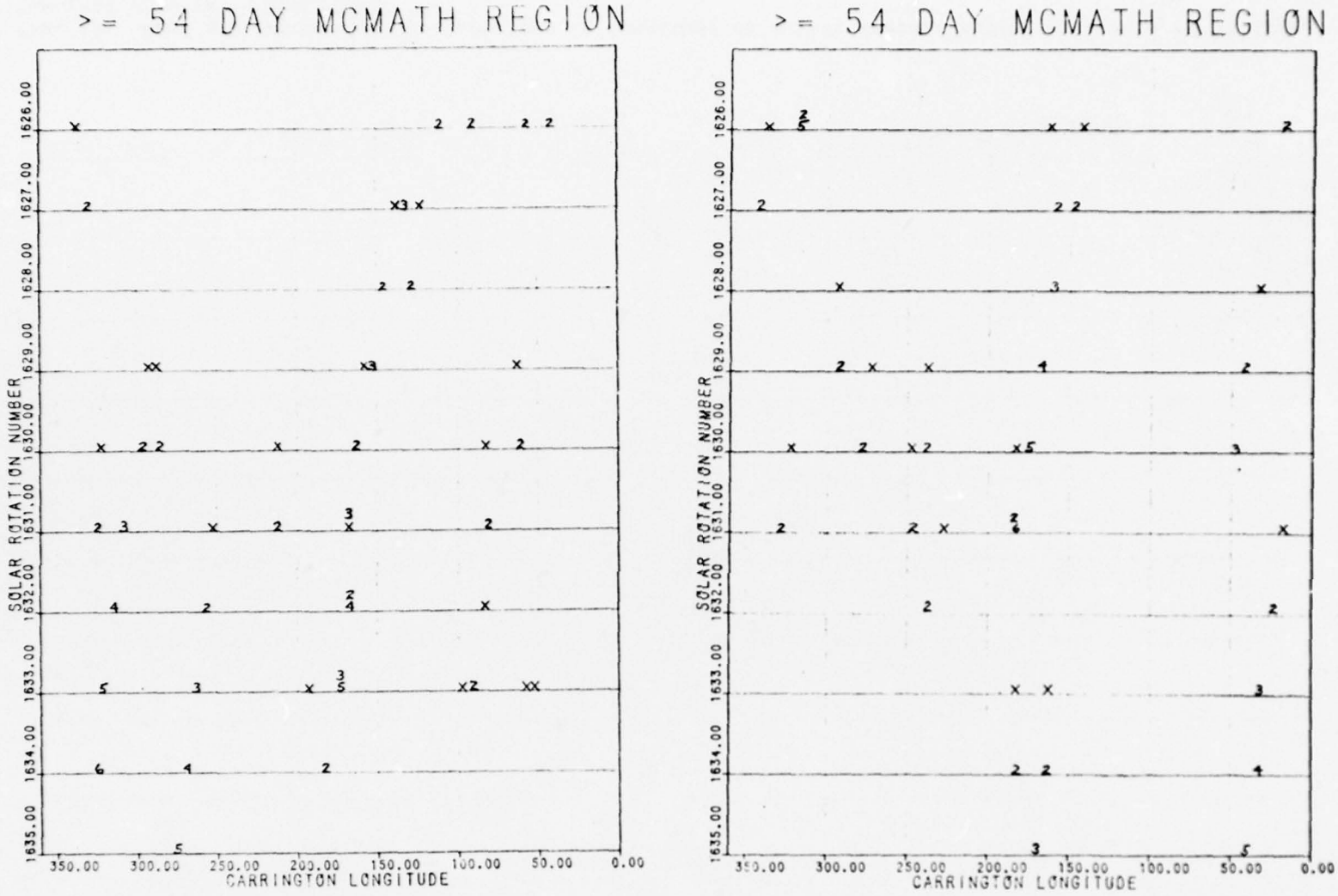

Fig. 15. A reproduction of Fig. 14 with each region replotted for each successive rotation that the region continues to be identifiable on the solar disk. The randomized data was also replotted using the same distribution of lifetimes possessed by the real regions. Real data on the left.

about future observations of ephemeral regions, the future course of solar activity in general, and to reinterpret data acquired in previous years (X-ray bright pt. and ephemeral region data).

In Fig. 16, we re-examine the latitude distribution of ephemeral regions for 1975, in comparison with similar distributions for 1970 and 1973. In retrospect we can now see evidence of high latitude maxima corresponding to the new solar cycle 21 both in 1973 and in 1970. During this 5 year interval these high latitude maxima seem to remain centered between 37° and 44° in both the northern and southern hemisphere. However, this does not mean that there is no equatorward progression of these maxima, although it does mean that possible equatorward progression would be slow, 1.4 degrees/year or less on average. Indeed, during this same interval in 1975, the equatorward progression of the low latitude maxima was slow -- about 1° per year as measured on a "butterfly diagram" (Fig. 18). Additional evidence that these high latitude maxima belong to incoming solar cycle 21, as far back as 1970, can be seen in Fig. 17. In Fig. 17 reverse orientation regions (i.e., reverse orientations to the Hale law of sunspot polarities for cycle 20) are subtracted from the proper polarity orientations and shown as a function of latitude. Low latitude regions have a dominance of properly oriented regions which changes to a dominance of reversely oriented regions between 18° and 30° north and south latitude. These first significant reversals of the dominant orientation occur in the northern hemisphere around 30°, 24°, and 18°, respectively, for 1970, 1973, and 1975. In the southern hemisphere the reversals occur around 24° during these periods. These reversals are just about halfway between the new and old cycle maxima in the latitude distribution. Poleward of these reversals in the dominant orientation regions may either be proper or reverse on average. The fluctuations in dominant orientation near the poles may be an indication that the poleward ephemeral regions are on average shorter-lived than the low latitude ephemeral regions. As illustrated in Fig. 5, the shortest-lived active regions tend to be more randomly oriented.

Now that we have evidence that ephemeral regions related to solar cycle 21 were present in significantly large numbers at middle and high latitudes in 1973, we can offer a reinterpretation of the x-ray bright points which are the x-ray counterpart to ephemeral regions. Upon examination of data taken by the S-054 x-ray experiment on board Skylab, Golub et al. (1975) have interpreted the total x-ray bright point distribution in latitude as consisting of the sum

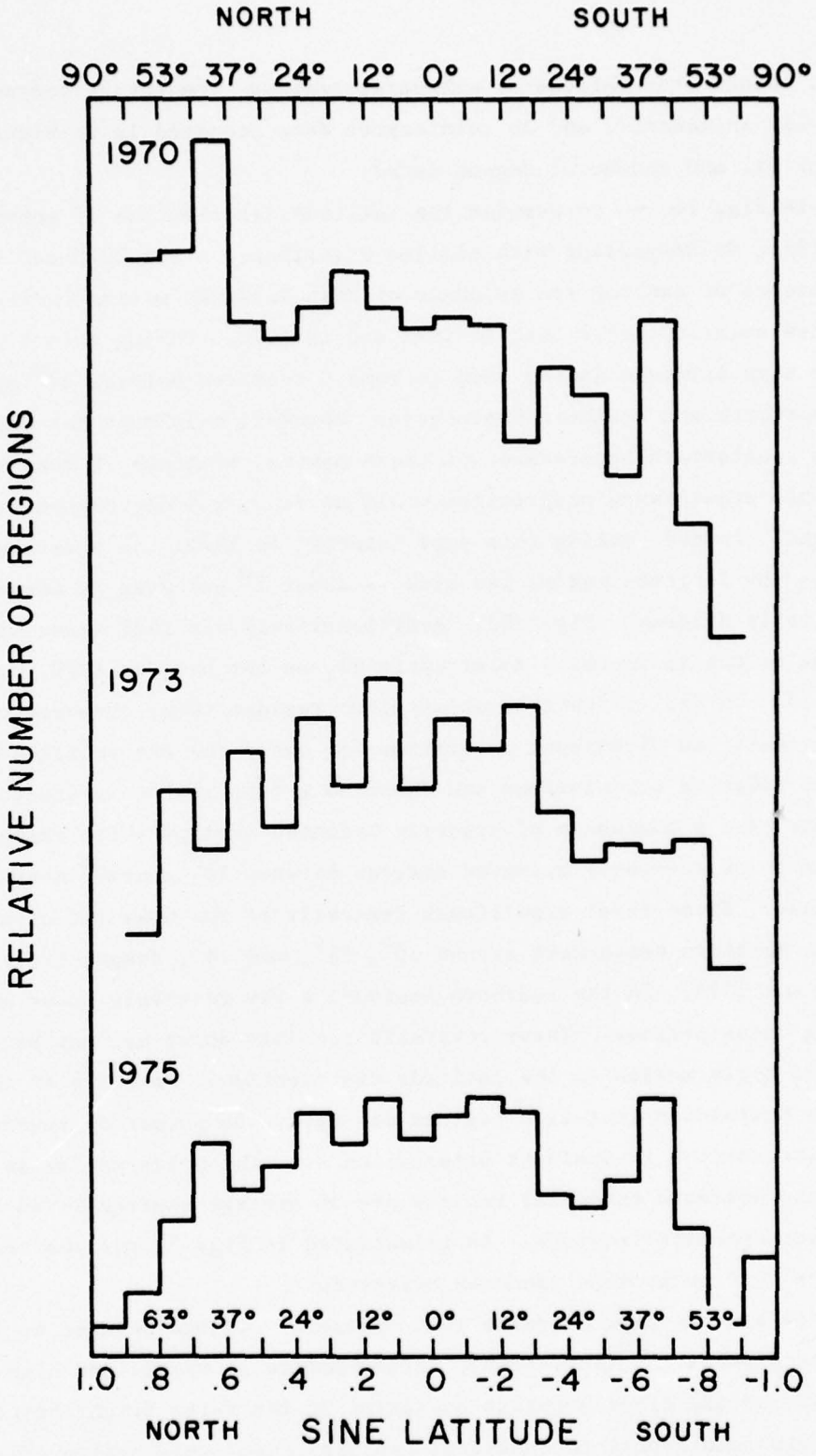

Fig. 16. A comparison of the latitude distributions of ephemeral regions for 6 month intervals in 1970, 1973, and 1975.

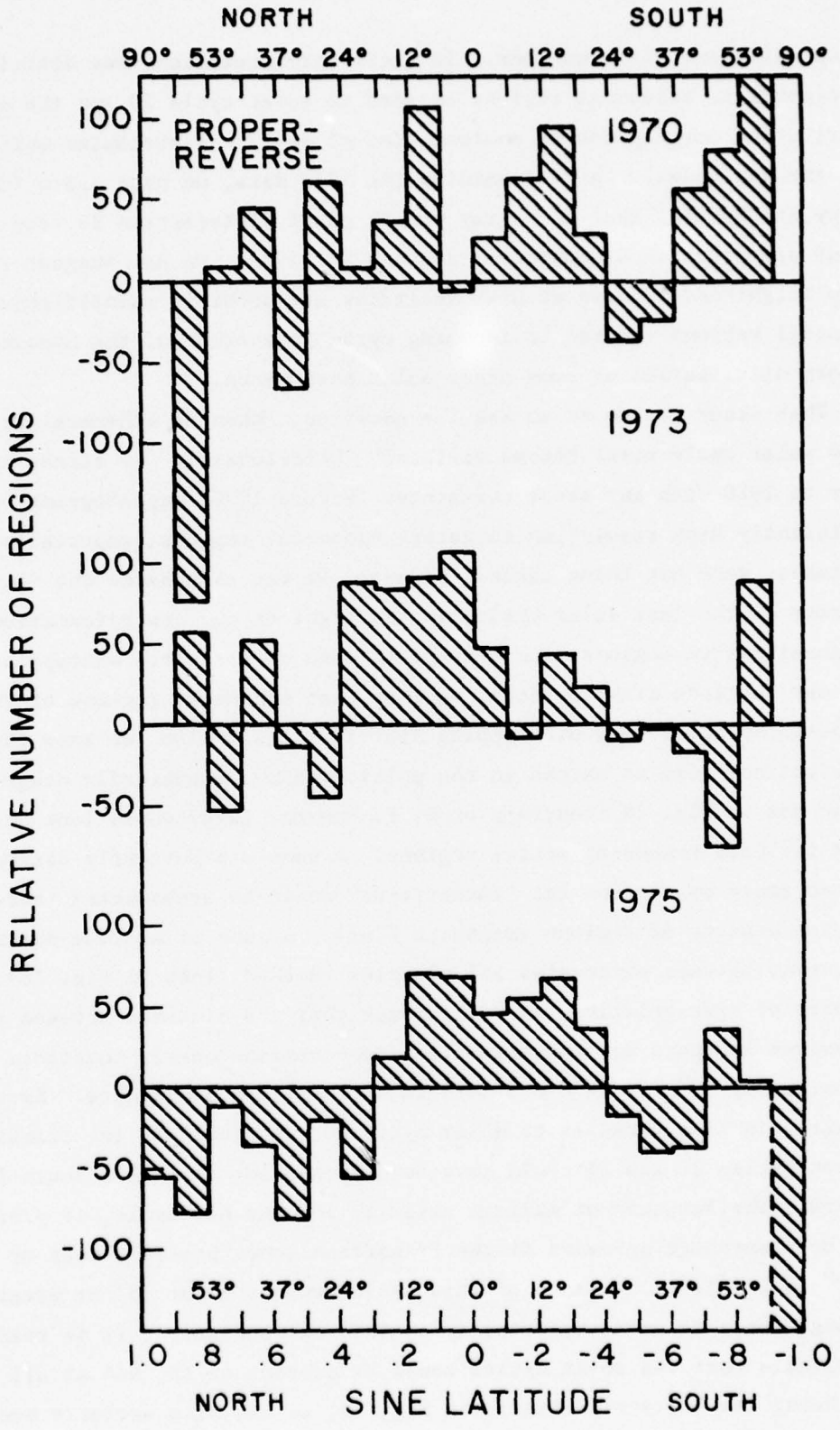

Fig. 17. Subtractions of the 'proper' and 'reverse' orientation categories of ephemeral active regions for 6 month intervals in 1970, 1973, and 1975.

of two different distributions. In their interpretation, one distribution corresponds to ephemeral regions related to solar cycle 20 and the other distribution corresponds to another kind of feature distributed uniformly over the whole sun. In re-examining the 1973 data, we note again (Harvey, Harvey and Martin) that the x-ray bright point distribution is very similar to our distribution of ephemeral regions for 1973. We now suggest that most x-ray bright points seen at high latitudes are probably identifiable with ephemeral regions related to incoming cycle 21 instead of the hypothesized uniform distribution of some other solar phenomenon.

This study causes us to ask the question, "When do ephemeral regions of a new solar cycle first become visible?" Unfortunately, we cannot extrapolate prior to 1970 with any great certainty. Before 1970, magnetograms of sufficiently high resolution to detect ephemeral regions, especially at high latitudes, were not being taken. However, we can re-examine the "butterfly" diagrams of the last solar cycle, in the light of our new information on ephemeral active regions, and attempt to make a reasonable extrapolation. From our latitude distributions, we know that ephemeral regions of the incoming and outgoing cycle have overlapping distributions. Also, we know that these distributions seem to extend to the poles. Hence, a butterfly diagram such as the one in Fig. 18 (courtesy of R. F. Howard, 1976) would look quite different if it included ephemeral active regions. A complete butterfly diagram would have no empty spaces and the "butterflies" would be areas where there would be a higher density of regions (magnetic flux). A zone of minimum density might be present between successive solar cycles (dashed lines in Fig. 18). For purposes of extrapolating, we will assume that the distance between the latitude of maximum sunspots and the transition zone remains nearly constant. It was approximately 17° for 1970 and 1973 in the northern hemisphere. Extrapolating backwards in time parallel to solar cycle 20, we find that the transition zone between cycles 20 and 21 could have been around 50° north and south latitude in 1966. The latitude of maximum activity for the new cycle, if present, could have been anywhere poleward of the transition zone, possibly near or poleward of 67° if the latitude range of this cycle remains about 35° or greater. Although there is great uncertainty in this extrapolation, it is readily conceivable that two solar cycles could be present on the sun at all times.

Using the butterfly diagram in Fig, 18, we can also estimate how long ephemeral regions belonging to solar cycle 20 will continue to be visible at

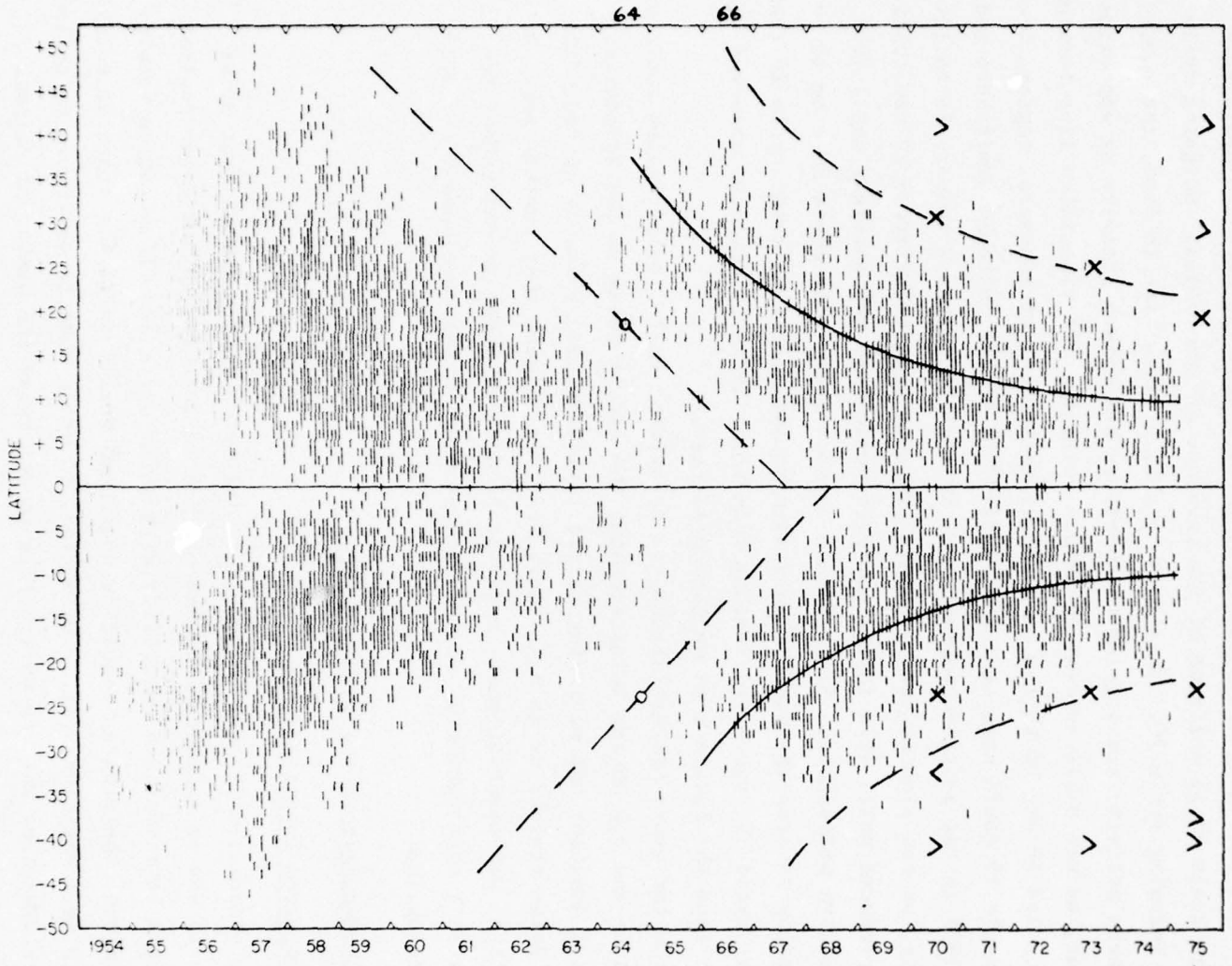

Fig. 18. "Butterfly diagram" showing the change in latitude of active regions over solar cycle 19 (1954-1965) and solar cycle 20 (1964-). Dashed lines and X's represent latitudes of the "transition zone" between adjacent cycles. Carats (>) represent maxima in ephemeral regions associated with the early development of solar cycle 22. (Butterfly diagram provided by R. F. Howard, Hale Observatories.)

near-equatorial latitudes. On the transition line (dashed line) between solar cycle 19 and 20, we can place points at N18 and S24 corresponding to the transition zones found for the 1975 data. We find that these points occur during 1964, one solar cycle earlier than 1975 when the northern hemisphere displays again clear evidence of the presence of two cycles: outgoing cycle 19 and incoming cycle 20. We also note that at this time in 1964, the southern hemisphere activity was lagging the northern hemisphere activity by approximately one year, as was still evident in 1975. Following the transition line between solar cycles 19 and 20 to the equator, we estimate that ephemeral regions from solar cycle 19 could have continued until 1967 in the northern hemisphere and until 1968 in the southern hemisphere. If 1975 activity is comparable to 1964 activity, we can predict that ephemeral regions from solar cycle 20 may continue to be produced until 1978 in the northern hemisphere and possibly until 1979 in the southern hemisphere. Since active regions from solar cycle 20 seem to be progressing towards the equator more asymptotically during solar cycle 20 than in solar cycle 19, ephemeral regions from solar cycle 20 could be observed even further into the future than we have predicted.

From the above extrapolations, it is evident that 3 solar cycles could be present on the sun during solar minimum: the oldest being in the equatorial region, a dominant one occurring at mid latitudes, and a new cycle beginning in the polar regions or at high latitudes. We suggest that further work, both theoretical and observational, needs to be done in order to understand the obvious roll that ephemeral regions are playing in the development and decay of solar cycles.

8. RECOMMENDATIONS FOR FUTURE STUDIES

Long-term Investigations

An observational program should be initiated during the current solar minimum to see if ephemeral regions can yet be detected in the polar regions or at high latitudes and identified with solar cycle 22. If negative results are obtained, the program should be continued yearly until the start of solar cycle 22 is identified. After detection, it would then be desirable to follow the development of the new solar cycle to determine the number of regions produced, the latitude spread, the rate of equatorial migration, and the extent to which the newest cycle overlaps in latitude with the active regions related to the dominant cycle (21).

Studies of ephemeral regions may yield important prognostic information on the course of solar cycles years in advance. A "Maunder minimum," in which long-lived sunspot producing regions are absent, could again occur in the future. Such a "Maunder minimum" might be predictable if enough information is collected on the early development of solar cycles through the study of the ephemeral component as well as the long-lived component of solar active regions.

It is evident from this study that a "Maunder minimum" does not necessarily mean an absence of the solar cycle. There could be solar cycles in which the total number of long-lived active regions is very much smaller than in recent cycles. In this case the solar cycle could continue much as we know it but only observable in the form of ephemeral active regions.

Short-term Investigations

Another area of investigation suggested by this study of ephemeral active regions is the extent to which solar flares are related to small and large active regions developing within existing active regions. As illustrated in Fig. 1, both ephemeral and long-lived active regions increase enormously during solar maximum. This greatly increases the probability for the interaction of separately developing active regions. Our suggested study of the relationship of solar flares to the interaction of regions should have two parts: (1) flares occurring in the immediate vicinity of newly observable magnetic flux and (2) flares which occur in the nearby vicinity of newly appearing flux. The time scales and precursors of these two subsets of flares could be quite different. This study could be initiated using the limited number of time-sequences of high resolution magnetograms that have been taken since 1969 at various U. S. solar observatories since about 1969.

New programs should be begun to obtain high resolution observations of the evolution of all components of the magnetic field in conjunction with high quality observation of flares at visible wavelength. There is hope that the study of the interaction of magnetic flux from separate active regions in various states of growth and decay may yield more specific information useful in flare prediction.

REFERENCES - Part I

Babcock, H. W.: 1961, Ap. J. 133, 572.

Golub, L., Krieger, A. S., and Vaiana, G. S.: 1975, Solar Phys. 42, 131.

Harvey, J. W., Harvey, K. L., and Martin, S. F.: 1975, Solar Phys. 40, 87.

Harvey, K. L. and Martin, S. F.: 1973, Solar Phys. 32, 389.

Leighton, R. B.: 1969, Ap. J. 156, 1.

Parker, E. N.: 1970, Ann. Rev. Astron. Ap. 8, 1.

Weart, S. R.: 1970, Astrophys. J. 162, 987.

Part II - Characteristics of Individual Ephemeral Active Regions

1. INTRODUCTION

It has become increasingly evident through our several studies of ephemeral active regions that their emergence is a frequent occurrence, and that these small bipolar regions are just small active regions. It is therefore probable that much of what we have learned and can learn about the birth of ephemeral regions may also be similar for the longer-lived active regions which are much more difficult to record at birth.

In our initial investigations of ephemeral active regions, we first observed and studied the birth of 8 of these small bipolar regions (Harvey and Martin, 1973). We found that these regions (1) had a total magnetic flux ($|\phi+| + |\phi-|$) of 10^{19} - 4.7 x 10^{20} Mx with average flux of 10^{20} Mx, (2) extended over 2-4 x 10^{4} km, (3) expanded with an average speed of 1 km s^{-1}, (4) first appeared in Hα about 30 minutes after the onset of the region, (5) developed adjacent to existing network fields, rather than co-spatial with the network.

In this part of our investigation we have concentrated on two areas of particular interest: (1) the details of the birth, development, and decay of ephemeral active regions, and (2) the location of ephemeral regions in relation to the supergranule, cell structure. These characteristics of ephemeral regions were studied using new observations covering larger areas of the quiet sun and having higher spatial and temporal resolution than the data used in our first study.

2. THE OBSERVATIONS

The time-sequence of magnetograms and velocitygrams analyzed in this study were taken during three periods of time and on two telescopes at the Kitt Peak National Observatory. All of the observations employed the 512-channel magnetograph described by Livingston et al. (1976). Our first set of data was taken during 1-3 October 1975 using the 512-channel magnetograph at the main McMath Telescope. This data permitted us to study the dissipation and development of magnetic flux with very high spatial resolution and magnetic sensitivity. The magnetic and velocity data covered an area 3.2 arc-min square at 7.5 minute intervals. The spatial resolution was 0".75. The second and third sets of observations were made at the Vacuum Telescope again using

the 512-channel magnetograph. During the periods of 19-22 November 1975 and 17 January 1976, we repeatedly observed an area 17.0 x 18.5 arc-min centered on the central meridian at intervals of 12.5 minutes. The spatial resolution of these data was 1".

For all of our observations, the spectral line Fe I 8688 Å was used to measure the magnetic and velocity fields. The instrumental noise level in the magnetic field data is 2 G per $(0\overset{''}{.}75)^2$ for the McMath data and 7 g per $(1'')^2$ for the Vacuum Telescope data. The data were taken at appropriate intervals of time to allow the subduing of the oscillatory velocity field when subsequent velocity pictures were added.

3. BIRTH, DEVELOPMENT AND DISSIPATION OF EPHEMERAL ACTIVE REGIONS

In Table 1, we have summarized the observations and the number of regions whose birth, development or decay were observed. During the three periods of observation 90 regions emerged; 37 more were observed in a developing phase; 77 were seen to decay or disappear. During the November period, the only period where the same area of the sun was observed on consecutive days, 23 regions were born overnight (included in the above tabulation of regions developing) and 23 regions disappeared overnight. Because of the large number of regions in our sample, we decided to restrict our present detailed analysis to the best data. This included the October 1975 data, January 1976 data, and some of the larger regions observed during November 1975.

3.1. Frequency of Occurrence of Ephemeral Regions

The appearance of ephemeral active regions is a very frequent occurrence. During the October period, for example, an average of 1 region emerged per hour per 10^{10} km^2. If this rate of region formation is typical of the low latitudes, 154 regions would emerge per hour between the latitudes N30 and S30 on the visible hemisphere of the sun during solar minimum. This is a factor of 26 greater than expected from the statistical analyses of the Kitt Peak daily magnetograms discussed in the previous part of this report (assumes an average region lifetime of 8 hours). It is also a factor of 4 greater than the rate of region occurrence observed with the Vacuum Telescope data taken on 17 January 1976, data which has slightly lower resolution and magnetic sensitivity. With better resolution and magnetically sensitive data, we observe more bipolar regions. As far as we can tell we have not resolved the smallest of these

Table 1

Date	Number of Regions				Observations			
1975	From Birth	Decaying	Born*	Decayed*	Area Km^2	Period Hrs.	Resolution Spatial, Arc-sec	Resolution Time, Min
Oct 1	12	9			1.9×10^{10}	4.8	.75	7.5
Oct 2	21	11			1.9×10^{10}	7.5	.75	7.5
Oct 3	11	17			1.9×10^{10}	8.0	.75	7.5
Nov 19	5	4		9	2.8×10^{11}	6.6	1	12.5
Nov 20	7	9	11	14	2.8×10^{11}	4.4	1	12.5
Nov 21	5	6	12		2.8×10^{11}	4.9	1	12.5
1976								
Jan 17	29	21			2.8×10^{11}	3.9	1	12.5
TOTAL	90	77	23	23				

*During November we observed the same area of the sun on consecutive days; these tabulations indicate the number of regions which formed or disappeared overnight.

bipolar regions, though perhaps the observations of Harvey and Livingston (1976) of bipolar elements located within supergranules have defined this limit.

3.3. Pre-region Effects Observed in the Network Fields

With few exceptions, ephemeral active regions affect and alter the existing surrounding network fields. This occurs at all stages of a region's development from just prior to emergence until its demise.

The changes in the network fields observed just prior to region emergence seem to occur in two forms: (1) the dissolution of existing network flux at the location the region is to emerge, and (2) the shifting of network elements away from the location of the emerging region.

The first change occurs when a region emerges precisely at the location of existing network, or in some cases, at the location of an existing bipolar region. As shown in Figure 1, prior to the appearance of Region B1, the network (black) begins to disappear. The disappearance of the network flux occurs regardless of the sense of the polarity of the part of the region emerging in the network in relation to the network polarity. The birth of a region in network fields does not seem to affect the subsequent development of the region.

In some instances a new region emerges at the location of an existing region, in which case we see the dissolution of the existing region, as for example Regions B2 and D1 in Figure 2. Invariably one polarity of the existing region will remain, though diminished from its original strength, as the new region begins to erupt. The left-over flux then appears to move to and join the new region flux as happened with the dissolution of Region D1 and the emergence of Region B2 (Figure 2).

The shifting of flux elements away from the location of the emerging region is not an infrequent occurrence. One example of this is shown in Figure 3. In the 10 to 15 minutes prior to the appearance of the emerging Region B5, a white flux element located just north of Region B5 shifts northward at a speed of 0.6 km s^{-1} towards a black flux element. In this particular instance, the motion of the network elements away from the emerging region appears to be along the supergranular boundary.

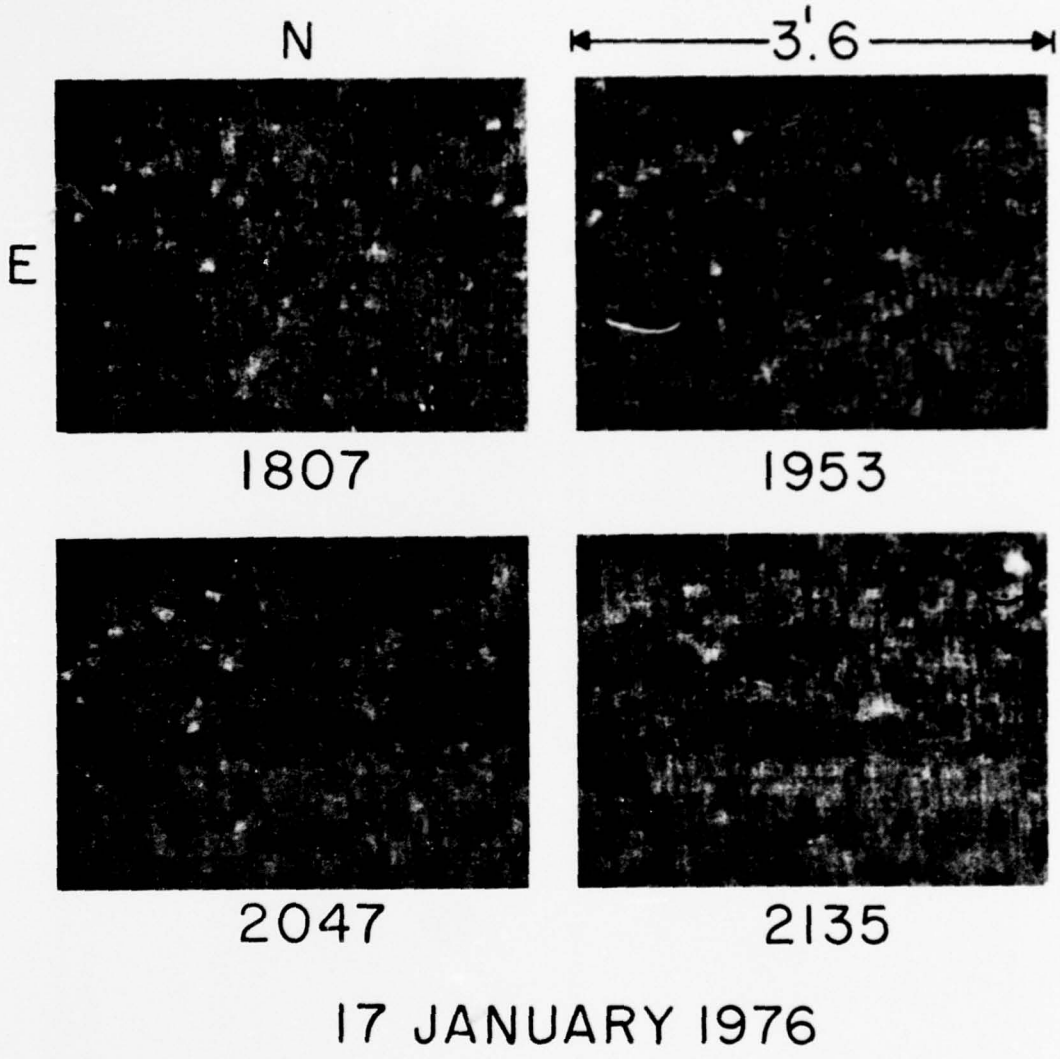

Fig. 1. Sequence of four magnetograms taken on 17 January 1976 showing the development of Region B1. Polarity of the magnetic field is represented by a departure to the black or white from grey.

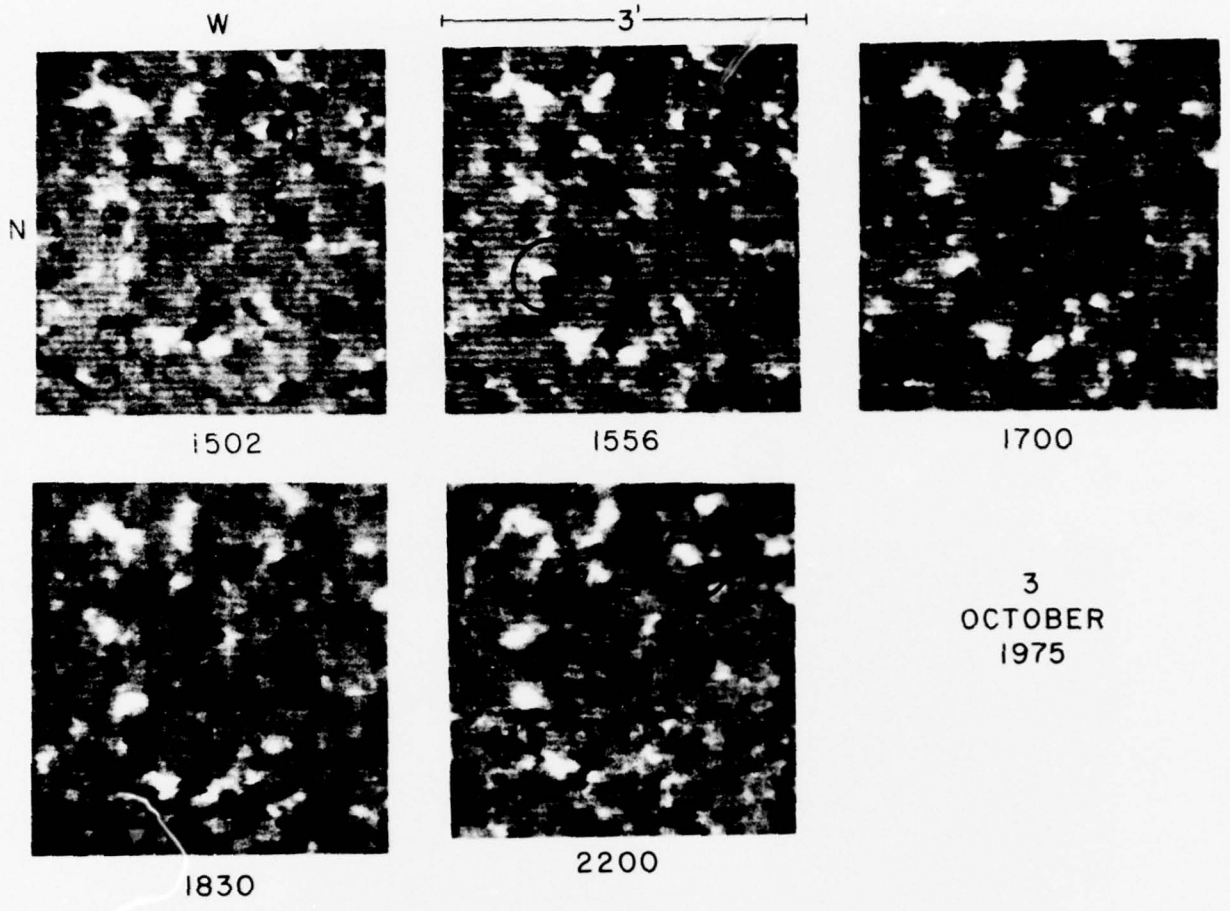

Fig. 2. Sequence of magnetograms shows the emergence and development of Region B7. Region D1 decayed prior to emergence of Region B2.

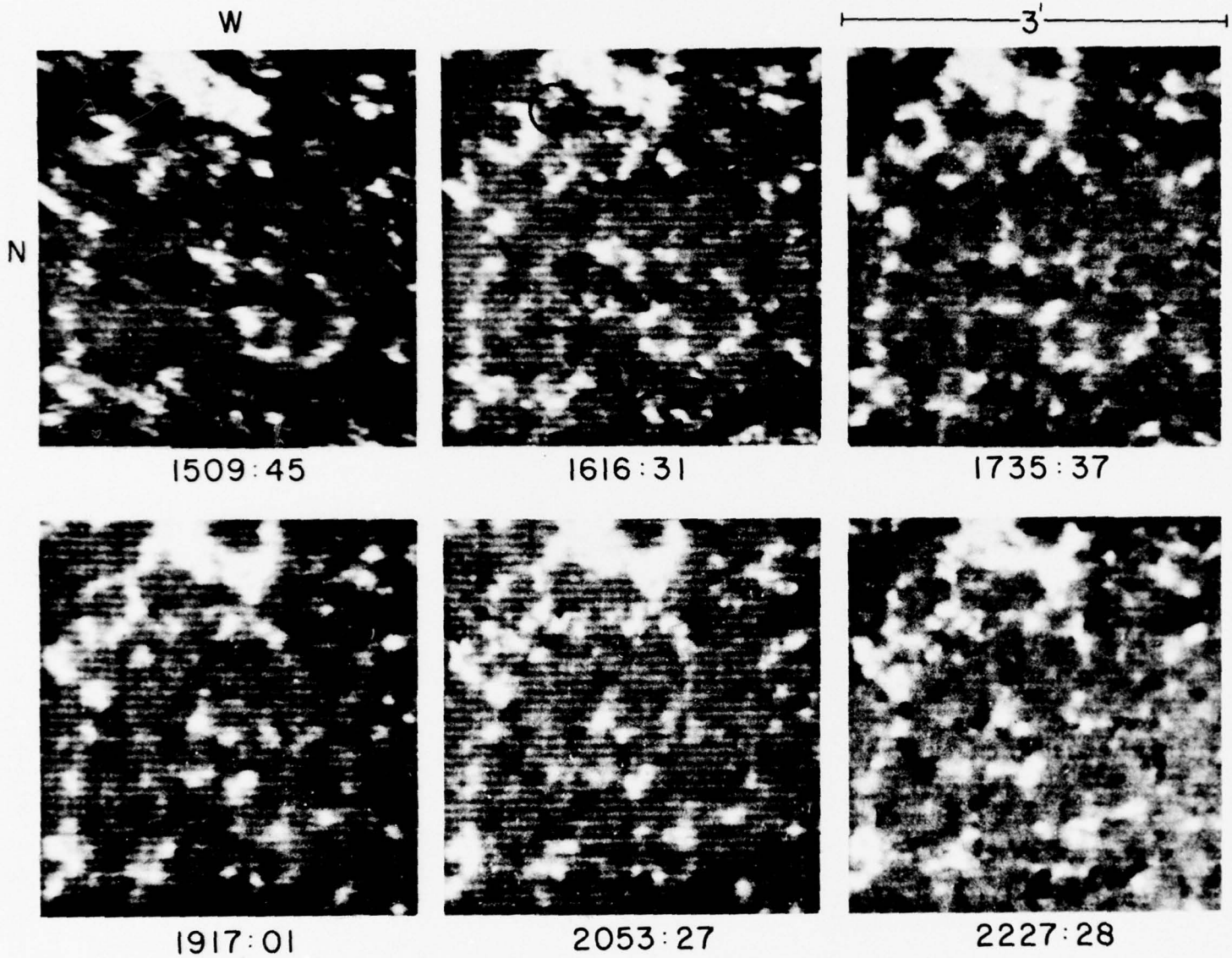

Fig. 3. Sequence of magnetograms taken on 2 October 1975 showing the birth and development of Regions B1, B5, B3 and B4 and the dissolution of Region D7. Note the expanding magnetic cells in the NW corner and in the central eastern part of the magnetograms.

3.3. Birth and Development of Ephemeral Regions

The regions we have studied seem to show no preferences as to their point of emergence in relation to the existing network fields. This is contrary to the conclusion of our first study but our sample of regions studied was small (Harvey and Martin, 1973) and to the observations of Zirin (1974).

We defined the 'start' of the region by extrapolating the growth curves of the magnetic flux, area and the border expansion to zero or to the background level. Our first observation of a region, i.e., when the longitudinal magnetic field of the region became measurable, occurs 10 to 20 minutes after the defined 'start' of the region. At this time a region is an average of 5" long, 4" wide and the opposite polarity peaks are separated by 2".6.

Figure 4 shows the rate of change of the total flux ($|\phi+| + |\phi-|$) and the expansion curves (of the peaks and the borders along the major axis) of 3 regions, Regions B1 shown in Figure 1 and B3 and B1 shown in Figure 3. Along the major axis of the region, the borders expand at rates of 1-3 km s^{-1}. Often the expansion of the major axis borders was constant, as for example Region B3 (2 October 1975) shown in Figure 3. In some regions, such as Region B1 (2 October 1975), the borders expand at an initially high rate during the first 30 minutes. During the subsequent development the rate of expansion decreases. The peaks of opposite polarity in the region separate at slower rates than is observed for the borders. The peak separation rates range from 0.7 - 1.7 km s^{-1}. The pattern of the peak separation does not necessarily mimic that displayed by the border expansion.

The maximum total flux ($|\phi+| + |\phi-|$) observed in the ephemeral regions studied showed a large range, 0.2 - 33 x 10^{19}Mx. The average total flux was 3.3 x 10^{19} Mx. A maximum in the total magnetic flux curve occurred during our observations for 95% of the emerging ephemeral regions and was reached from 0.7 to 3.5 hours after the 'start' of the region.

During the growth of the emerging regions, the flux density (total magnetic flux/area) was found to increase by 10 to 60 G indicating that we were observing the emergence of subsurface fields. The maximum flux densities determined for the growing region ranged from 25 - 90 G.

The flux increases generally were linear if the region had a fairly simple bipole configuration during its emergence and development, such as Region B1 (2 October 1975, Figures 3 and 4). Region B1 (17 January 1976), shown in Figure 1, illustrates an example of non-linear development in a region. The

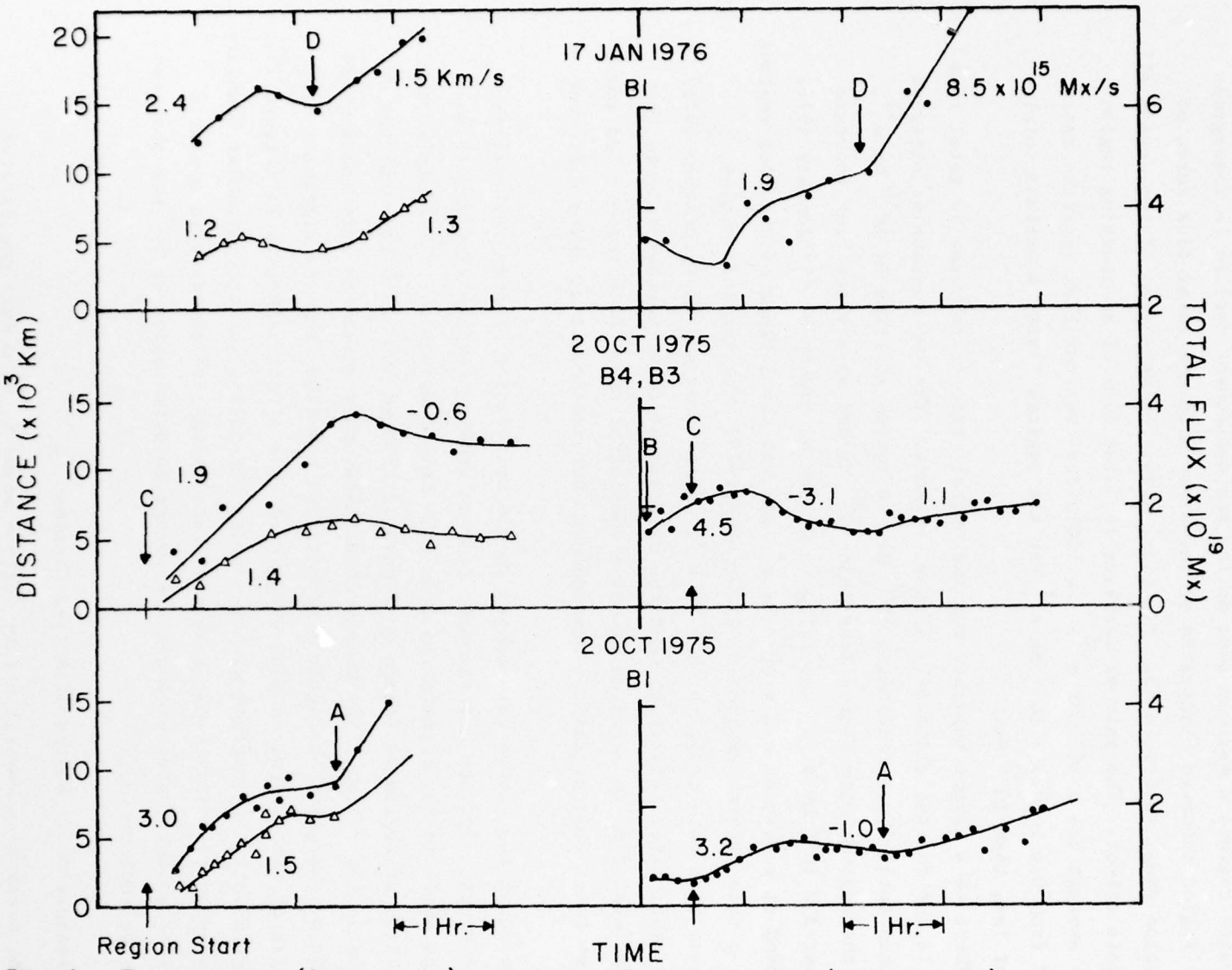

Fig. 4. The expansion (left graphs) and the total magnetic flux (right graphs) curves for 4 emerging ephemeral regions. Separation of borders along major axis represented by dots (•). Separation of peak fields shown by triangles (△). Lower Graph: Region B1 (2 October 1975). Middle Graphs: Regions B3 and B4 (2 October 1975). Top Graph: Region B1 (17 January 1976). The expansion rates are indicated adjacent to each expansion curve and arc in km s^{-1}. Similarly, the rates of flux increase are indicated and are in 10^{15} Mx s^{-1}. A: at this point in the decay of Region B1 the flux elements of an expanding magnetic cell entered the area occupied by the region. B: Region B4 is growing when we first observe it. C: the 'start' of Region B3; the decay of Region B4 follows shortly after. D: eruption of new flux in Region B1.

initial emergence of the region was a simple bipole; the growth curves show a linear increase in the measured parameters of the region. Within 40 minutes the region reached a maximum and, during the subsequent decline, a resurgence of the region occurred (indicated by the arrow *D* on the total flux curve of the region shown in Figure 4). The flux, area, and expansion of the region all show this effect. The rate of increase in total flux of an emerging region was an average 3.4×10^{15} Mx s^{-1}. In individual regions flux increase rates ranged from 0.6 to 7.4×10^{15} Mx s^{-1} for the regions having a maximum total flux of less than 10^{20} Mx.

There is a slight tendency for the overall rate of increase in total flux to be larger for the ultimately larger regions. The two regions we observed, which had total fluxes exceeding 10^{20} Mx, increased at rates of 10^{16} Mx s^{-1}, while the regions with fluxes less than 10^{20} Mx had an average flux increase of about 3×10^{15} Mx s^{-1}. Referring to Figure 4, Region B1 (17 January 1976) increased at a rate of 8.5×10^{15} Mx s^{-1} and was the largest of the four regions shown in this Figure. Region B1 (2 October 1975), the smallest region, increased at a rate of 3.2×10^{15} Mx s^{-1}. Regions B3 and B4 (2 October 1975), on the other hand, illustrate that the relation of flux increase rate to the maximum total flux of a region is not a consistent one. Both regions had about the same total flux at maximum development, but reached it at quite different rates.

We found two causes for changes in the orientation of emerging regions. (1) The eruption of new and stronger flux in growing regions resulted in an apparent shift in the orientation from that held previously. For example, the orientation of Region B1 (shown in Figure 1) changed 100° with the eruption of new flux in the region. (2) On the other hand, many instances were found where significant changes in a region's orientation resulted from the migration of the poles of the region. A good example of this effect is Region B5 (Figure 3). The region initially emerged with its poles straddling the supergranular boundary. The two opposite polarity poles then migrated along the boundary is opposite directions as the region expanded. A change in orientation of 60° was observed over a two hour period.

3.4. Dissipation of Ephemeral Active Regions

The decay of ephemeral active regions seems to be a more complicated process than the birth and therefore the interpretation of what we are seeing

is more difficult. During both the development and decaying phases, regions are influenced by the motions of and interactions with the network fields whereas during their initial eruption, this did not appear to be the case.

When a region is observed at birth or throughout most of its lifecycle, it is obviously a bipolar unit. However, where we have not observed the emerging or growing phase, identification of a bipolar unit is not as easy due to the proximity of network fields. Our selection of decaying regions, therefore, was based on what we have learned about regions where most or all of the lifecycle has been observed and on the behavior of opposite polarity elements in close proximity.

We have noted several conditions under which flux was observed to dissipate or diminish. Some regions were observed to merge with surrounding network fields, either adding to the network flux when of the same polarity or diminishing it when of opposite polarity. An example of this behavior is Region B7 (3 October 1975) in Figure 2 and Region B1 (2 October 1975) in Figure 3. Both regions, after their emergence, separated with the poles moving towards and into neighboring network fields.

In another case, the eruption of a new ephemeral region in the vicinity of an existing small bipolar region resulted in the demise of the existing bipolar region. This occurred in the area marked B3-B4-D7 on Figure 3. Region B4 was growing at the beginning of our observations (see the total flux curve for Regions B3 and B4 in Figure 4). About the time Region B3 appeared, Region B4 began to decay. As B3 expanded it apparently forced Region B4 into what we have defined as a bipolar region D7. The positive (black) pole of D7 and Region B4 disappeared, leaving the negative (white) pole of D7. The negative pole of D7 later disappeared when it was caught between the positive pole of Region B3 expanding from the north and inflowing positive flux elements from the south. The flux curves of Region D7 are shown in Figure 5.

The flow of flux elements into an ephemeral region resulting in the partial disappearance of the region (and in some cases the addition of flux to the region) has been observed in several cases, as for example, described above. These flux elements are invariably small and do not cause the complete disappearance of the region.

In only a few cases have we observed flux dissipation which resembles in appearance the reverse of the birth process of a region. The poles of a region move together at a rate of about 0.3 km s^{-1} while the flux and area is observed

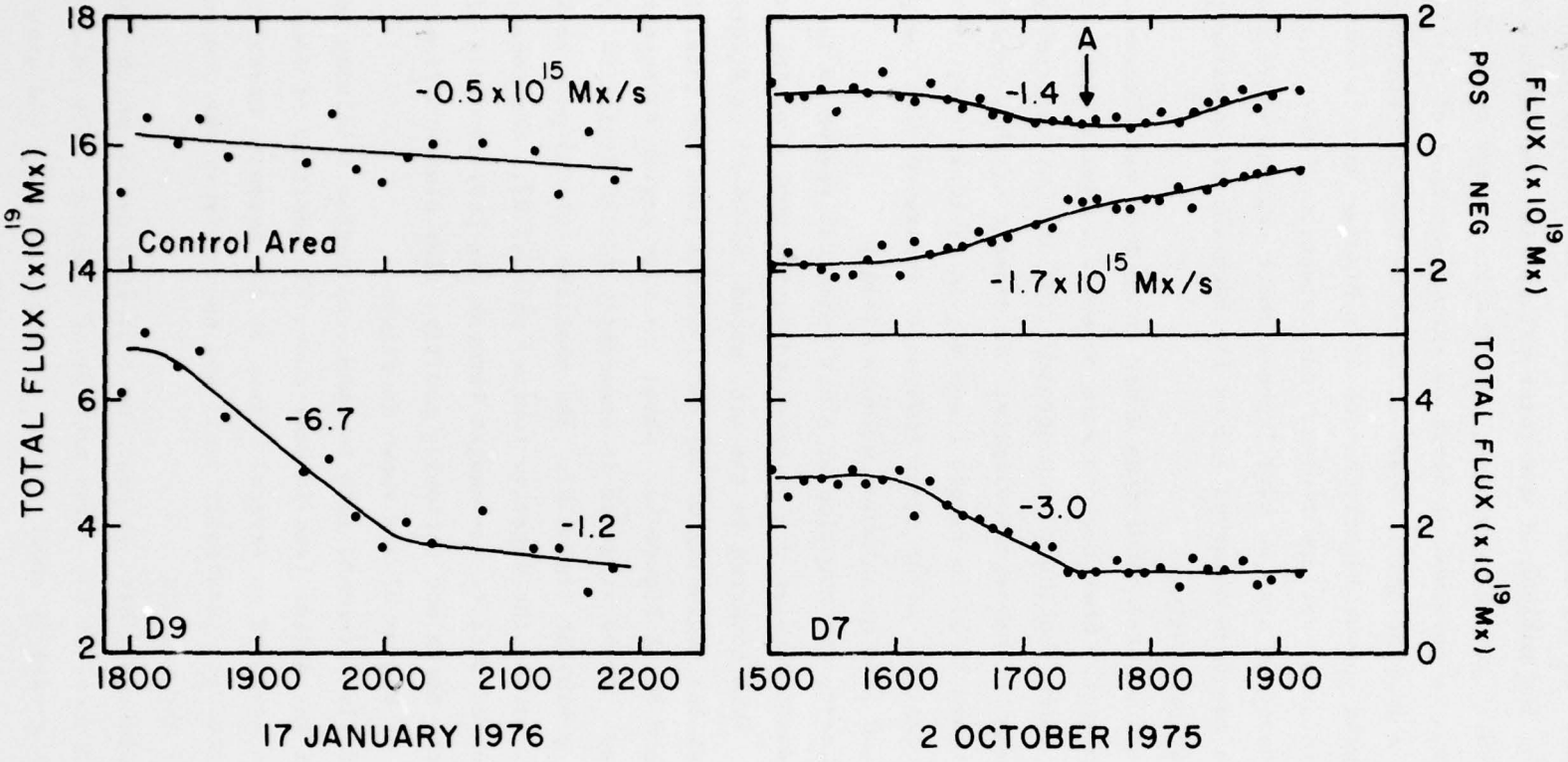

Fig. 5. Total flux curves during the decay phase of two regions, D9 (17 January 1976) and D7 (2 October 1976). Left Graph: Total flux curve of Region D9 and an adjacent Control Area. Right Graphs: Total flux and the positive and negative flux curves are shown separately of Region D7. At A growing Region B3 has expanded into the area previously occupied by Region D7. Slopes of the flux curves are in 10^{15} Mx s^{-1}.

to decrease. Region D9 in Figure 6 illustrates this type of flux decay. The total flux curve of Region D9 is shown in Figure 5 in relation to the total flux curve of a neighboring control area of flux. The flux of Region D9 is initially decreasing at a rate of -6.7×10^{15} Mx s^{-1} and slows to a rate of -1.2×10^{15} Mx s^{-1}. These rates are compared with a decrease of 0.5×10^{15} Mx s^{-1} in the control area. When first observed Region D9 had a bipolar magnetic field configuration with two strong peaks detected in the negative pole and one peak in the positive pole of the region. During the region decay, the northernmost peak appeared to shift towards the positive pole and away from the other negative peak and to diminish in strength. During this period, the positive pole also showed a decrease in flux, though it was not as large as measured in the decaying negative pole. A rotation of 110° of this pole about the positive pole was observed during the time of decay. 2.5 hours after our initial observation of this region the decaying negative peak was no longer detected and the region flux (total) had diminished 3×10^{19} Mx. The decay of one peak in a pole of a region, particularly if it is the strong peak, can result in an apparent change in orientation of a region, through this was not the case in Region D9.

The decay rates of the flux regions studied ranged from -0.7 to -8×10^{15} Mx s^{-1}, the average being -2.9×10^{15} Mx s^{-1}. When we compare this rate to the rate at which flux emerges, we find that within the noise level of our data flux disappears at the same rate as it erupts.

3.5. Lifetimes of Ephemeral Active Regions

The lifetimes of the ephemeral regions we have studied in detail vary from as short as 2 hours to as long as 2 days. Only 35% of the 35 emerging regions and 5% of the 29 emerging regions identified during the October 1975 and January 1976 periods, respectively, were followed through their complete lifecycle (from their birth to their disappearance or until they were unrecognizable as a region). The lifetimes of these regions ranged from 2 to 7 hours. The total magnetic flux of these short-lived regions is less than 10^{19}Mx, where the average total flux of the regions we studied was 3.3×10^{19} Mx. For a few of the ephemeral regions, which were decaying but did not disappear, we estimated the lifetime by extrapolating forward the total flux curve at its rate of change in the decaying phase. Lifetimes of 10 regions determined in this way range from 4 to 16 hours.

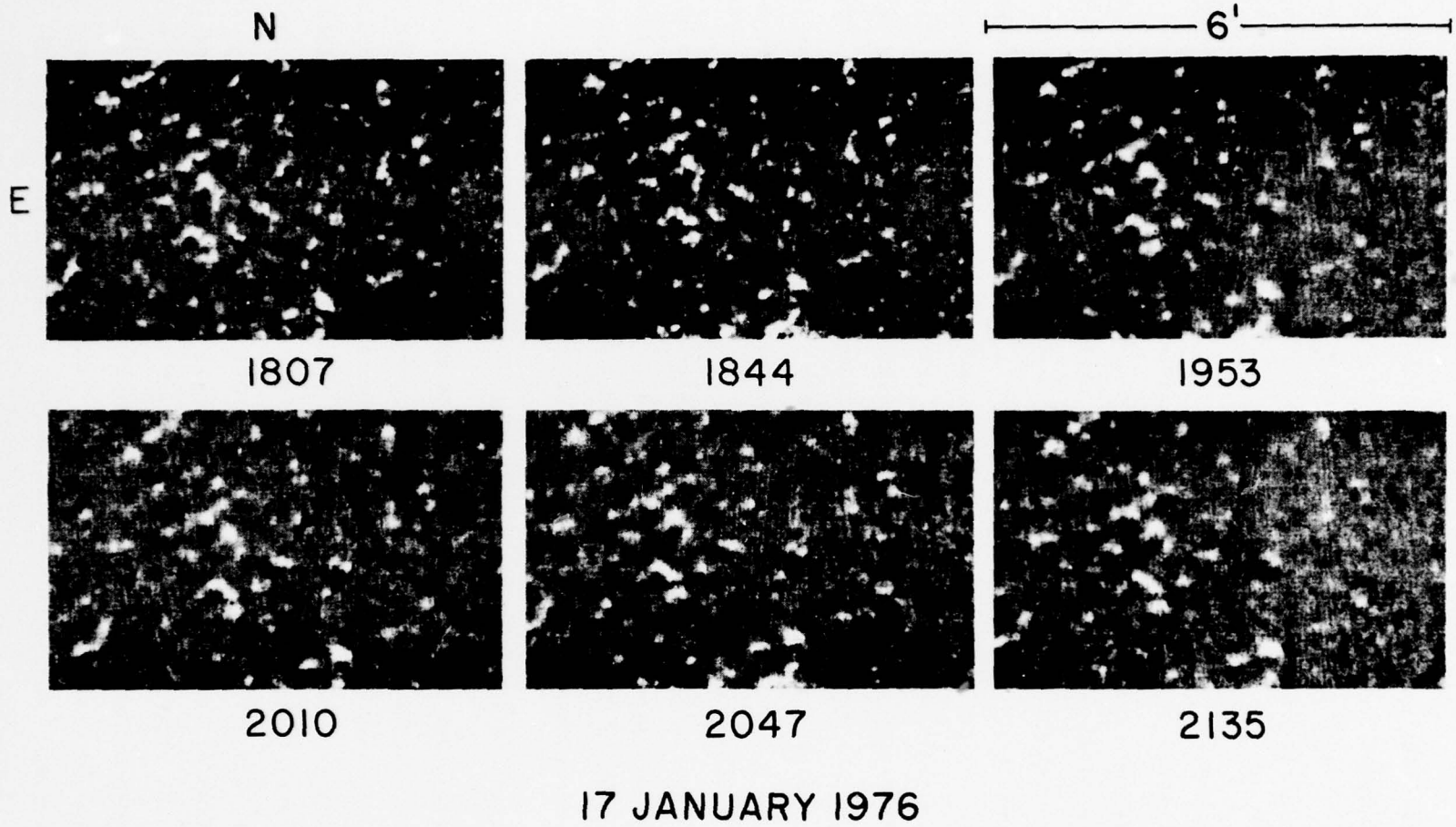

Fig. 6. Sequence of magnetograms taken on 17 January 1976 showing the decay of Region D9.

There does appear to be a rough correlation between a region's lifetime and its maximum total magnetic flux. The smaller the total magnetic flux the shorter the region's lifetime. Conversely, the more total magnetic flux in the region the longer the region will remain visible. The relation between a region's peak magnetic flux and lifetime for these sized regions is complicated, however, by the interaction of the region with surrounding existing network fields or by the emergence of other ephemeral regions close by. For example, the development of Region B4 (2 October 1975) shown in Figure 3 was arrested and, in fact, reversed coincident with the emergence of Region B3 and the interaction with another adjacent Region D7.

4. SUPERGRANULATION, NETWORK FIELDS, AND EPHEMERAL ACTIVE REGIONS

4.1. The Relation of Ephemeral Regions to Supergranule Cells

In this phase of our study we have investigated the relation between the sites of emerging and decaying ephemeral regions and the supergranular cell boundaries. Bumba and Howard (1965) first noted that active regions emerged at the vertices where two or more supergranule cells meet. This observation was further substantiated by Bappu et al. (1968) and Bumba et al. (1968). In these studies use has been made of Ca II emission network to define the supergranular pattern.

The problems in defining the supergranule cell pattern using the magnetic field pattern (and consequently the corresponding Ca II emission network) is illustrated by Figure 7. On each day of the October 1975 run, a sequence of magnetograms was made on a different area of the sun, each area quite different from that observed on the other two days. On 1 October, the area we observed was located in an old active region. As can be seen by a comparison of the magnetograms taken at the beginning and end of the day, the magnetic field pattern changes very little. It is possible to outline the supergranule cells since there exists a great deal of magnetic field network structure. On the next two days of observation, the reliability of such a procedure drops dramatically. On 2 October, at a location near the boundary of the old active region observed the previous day, there is not enough network field to reliably establish the pattern of supergranular cells. On 3 October, at a location within a coronal hole, the problem is hopeless. Therefore, it is necessary to determine the supergranular cell pattern by measuring and analyzing the velocity field.

In order to determine the supergranule velocity pattern, our observations were taken at intervals of time such that, when subsequent velocitygrams were added together, the effects of the oscillatory velocity field would be minimized and the supergranule velocity pattern enhanced. Our observations were also offset from the disk center so that the horizontal velocity flow of the supergranules could be measured. Figure 8 shows the average background velocity pattern observed on 2 October 1975. The supergranules show a pattern of black (velocity toward the observer) in the western part of the cells and white (velocity away from the observer) in the eastern portion of the cells. Overlaid on the velocity picture in the lower half of Fig. 8 is the pattern of cell boundaries we have determined using apparent motions seen when projecting the magnetic field data as a time-lapse film. The locations of region emergence are indicated

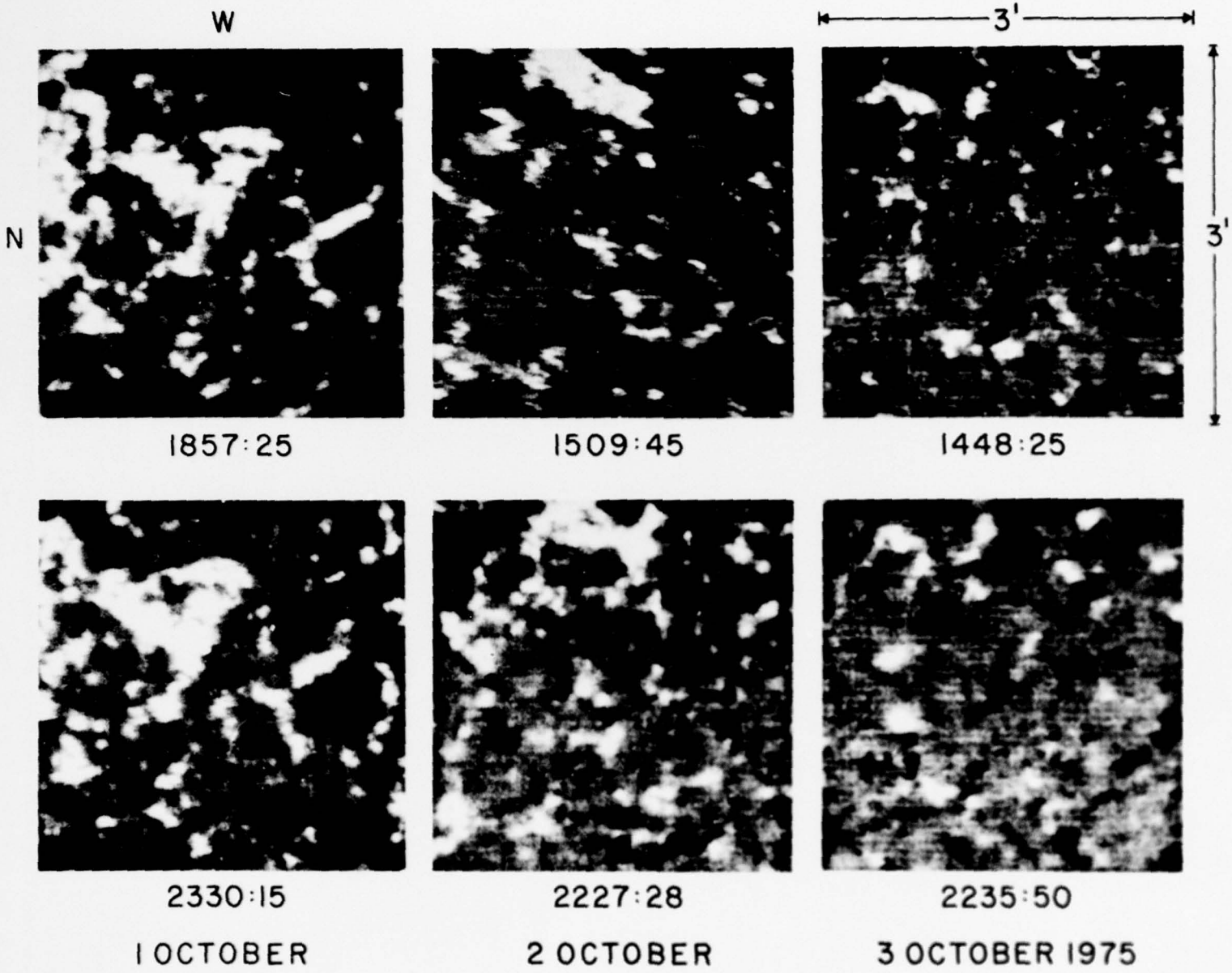

Fig. 7. Magnetograms from the beginning and end of observations on 1, 2 and 3 October 1975. 1 October: located in an old active region. 2 October: near the boundary of the old active region observed the previous day. 3 October: in a coronal hole.

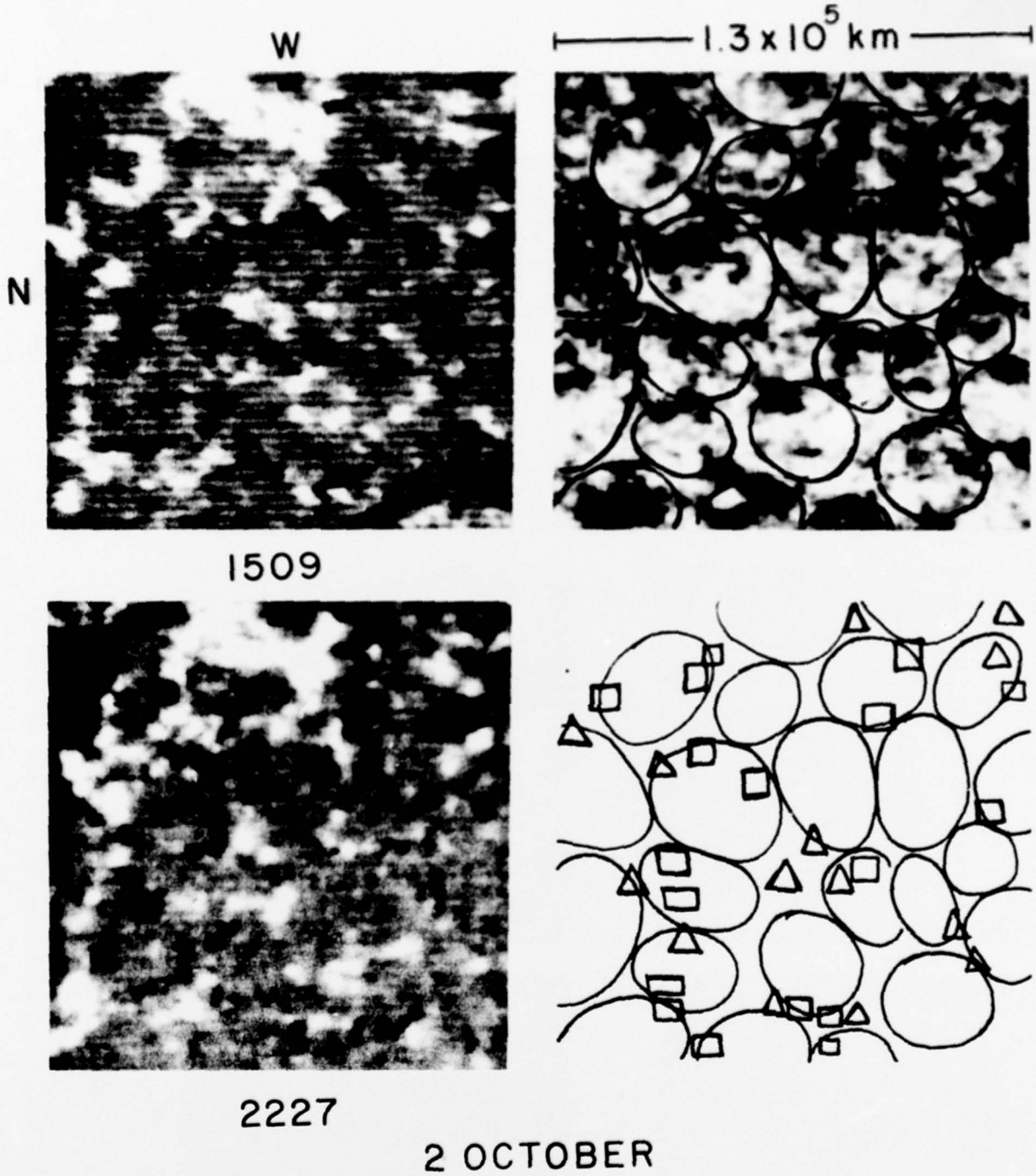

Fig. 8. Left: two magnetograms taken near the beginning and end of observing on 2 October 1975. Solid arrows indicate expanding magnetic cells. Dashed arrows indicate focal points of inflowing flux elements. Right: top picture is the average of velocity data over a 4 hour period (1554-2001). The deduced supergranule boundaries are shown superimposed. Bottom picture shows a composite of the deduced supergranule boundaries and the locations of emerging regions (□) and decaying regions (△).

by squares and region decay by triangles. Two magnetograms taken at the beginning and at the end of our observations are also shown.

It is apparent from Figure 8 that almost all of the emerging and decaying bipolar regions occur at or near the boundaries of supergranule velocity cells. The regions emerged with fairly random orientations relative to the boundary of supergranules. As the regions expanded, the motions of the region's poles was invariably along the supergranular boundary. This sometimes resulted in significant changes in the orientation of the region, as for example in Region B5 (Figure 3). It emerged at a boundary with an initial orientation of about 60° to the supergranule boundary. Over a period of 2 hours the region rotated in a counterclockwise direction until the region was aligned along the supergranule boundary.

Although elements of the magnetic network may be altered by the emergence of ephemeral regions and conversely, we have not yet seen evidence that the supergranule velocity pattern changed due to the eruption of the small bipolar regions. The supergranule cells deduced from velocity pictures taken at the beginning and at the end of our observations show roughly the same distribution over the area observed. However, Worden (1975) has observed changes in the velocity flow with the emergence of new flux.

4.2. Motions associated with Magnetic Network

The velocities observed at the location of network fields was consistently downward in accord with the results of Tanenbaum et al. (1969), Frazier (1970), Musman and Rust (1970), Deubner (1971) and Worden (1975). The motions of the network fields and of the regions (when occurring) were consistent with the deduced supergranular velocity cell flow. These motions were either along the cell boundaries or towards the boundary. In addition to ephemeral region expansion along supergranule boundaries, there were instances of network field similarly moving. For example, patches of field of both polarities were seen to move from the west into the strong network (white) structure located at the western edge of the magnetograms (Figures 3 and 8). The path followed by the moving network appears to be along a supergranule cell boundary.

The best examples of the effect of supergranule cell motion on the magnetic network motion towards a cell boundary are the expanding magnetic cells indicated by arrows in Figure 8 (see also Figure 3). However, only one expanding network cell, located in the NW corner of the magnetograms, showed a corresponding

velocity cell. The supergranular velocity cell was larger than the magnetic network cell and only showed up on the 4 hour composite velocity picture shown in Figure 8. The speeds of individual flux elements ranged from 0.3 to 0.5 km s^{-1}, consistent with observed horizontal velocities in supergranules. The other expanding magnetic cell showed no corresponding velocity cell. It was, in fact, centered on the boundary between two supergranule cells. The velocities of flux elements in this magnetic cell also measured between 0.3 and 0.5 km s^{-1}.

One other interesting feature found in these data was the motion of flux elements of both polarities from all directions into a small area. The two such areas found in the 2 October 1975 data are indicated by dashed arrows on Figure 8. This phenomenon continued throughout a day's observation. Flux was not observed to accumulate at the focal point of the moving flux; rather we saw the disappearance of flux elements at these locations. In each instance the focal point of the inflowing flux elements was located at the junction of at least 3 supergranules.

4.3. Discussion

It now appears that the principal difference between the bipolar regions we have studied and the larger active regions is the total amount of flux available to the region during its development and the subsequent modification, if any, to the supergranulation velocity pattern. Active Regions can be divided into 3 broad groups distinguished by their size relative to supergranulation cells. Most of the regions we have studied are less than 20,000 km at maximum development, that is, smaller than the surrounding supergranular cells. Their total fluxes are less than 10^{20} Mx; their lifetimes are 2-16 hours long. These regions do not appear to alter the existing supergranulation velocity cells. The next larger regions have fluxes in excess of 10^{20} Mx, extend over 30,000 to 40,000 km (comparable to the size of supergranules) and have lifetimes of 1-4 days. These regions appear to occupy a supergranule cell and have lifetimes comparable to the lifetime of a supergranule of $36\ ^{+70}_{-12}$ hours (Worden, 1975). The largest Active Regions typically have total fluxes of about 2×10^{22} Mx (Sheeley, 1966), span over many supergranule cells and have lifetimes from several days to several weeks. These regions very likely modify the pre-existing supergranulation velocity pattern. These divisions, although convenient in describing regions, are arbitrary since the sizes and lifetimes of active regions form a continuous spectrum from the largest and longest lived to the smallest and shortest lived.

5. CONCLUSIONS

To date our study has yielded the following results:

(1) The birth and decay of ephemeral active regions is a frequent occurrence. As many as 300 regions were estimated to form per hour in the sunspot zone (N30 to S30) during the solar minimum.

(2) Ephemeral active regions appear to alter the details of the existing network fields by moving network flux elements, adding to the network flux, and dissipating the network flux (and consequently, some of the region flux).

(3) The rate of flux increase (3.4×10^{15} Mx s^{-1}) is comparable to the rate of flux decrease (-2.9×10^{15} Mx s^{-1}) in these small bipolar regions.

(4) Ephemeral active regions appear and disappear near the boundaries of the supergranule velocity cells, but they do not appear to modify the velocity pattern. Motions of ephemeral region components were observed parallel to the cell boundaries.

(5) Ephemeral region decay was complicated process, being strongly influenced by the neighboring network fields. The decay of regions appeared to result from the expansion into and absorption by network field, the emergence of a new ephemeral region in close proximity, the flow of network flux into the region, or by the merging and disappearance of small elements of opposite polarity.

(6) In time-lapse projection of our magnetic field data, we have observed expanding cells of network fields, junctures at network cell boundaries where fields disappear, and apparent motion of weak intercellular fields toward network cell boundaries.

6. RECOMMENDATIONS FOR FUTURE WORK

The speculation that the difference between small bipolar regions and the large active regions is in the amount of flux available to a region during its growth should be verified or negated by future observations of the birth of large regions.

High resolution observations in the polar regions and sunspot zones would be of value in determining the rate of formation of ephemeral active regions as a function of latitude. In addition, higher sensitivity magnetic field observations than used for this study are needed to better define the spectrum of active regions and the space occupied by them in the solar atmosphere.

7. REFERENCES - Part II

Bappu, M. K. V., Grigerjev, V. M., and Stepanov, V. E.: 1968, Solar Phys. 4, 409.

Bumba, V. and Howard, R.: 1965, Astrophys. 141, 1492.

Bumba, V., Howard, R., Martres, M.-J., and Soru-Iscovici, I.: 1968, in K. O. Kiepenheuer (ed.), 'Structure and Development of Solar Active Regions', IAU Symp. 35, 13.

Deubner, F.-L.: 1971, Solar Phys. 17, 6.

Frazier, E. N.; 1970, Solar Phys. 14, 89.

Frazier, E. N.: 1972, Solar Phys. 26, 130.

Harvey, K. L. and Martin, S. F.: 1973, Solar Phys. 32, 389.

Livingston, W. C. and Harvey, J. W.: 1975, Bull. Amer. Astron. Soc. 7, 346.

Livingston, W. C., Harvey, J., Slaughter, C., and Trumbo, D.: 1976, Appl. Optics 15, 40.

Musman, S. and Rust, D. M.: 1970, Solar Phys. 13, 261.

Sheeley, N. R., Jr.: 1966, Astrophys. J. 144, 723.

Tanenbaum, A. S., Wilcox, J. M., Frazier, E. N., and Howard, R.: 1969, Solar Phys. 9, 328.

Worden, S. P.: 1975, 'Solar Supergranulation', Ph.D. Thesis, University of Arizona, p. 57.

Zirin, H.: 1974, in R. Grant Athay (ed.),'Chromospheric Fine Structure', IAU Symp. 56, p. 161.